Atmospheric Environment 45 (2011) 4470–4480

Contents lists available at ScienceDirect

Atmospheric Environment

journal homepage: www.elsevier.com/locate/atmosenv

Concentrations of fine, ultrafine, and black carbon particles in auto-rickshaws in New Delhi, India

Joshua S. Apte [a], Thomas W. Kirchstetter [b], Alexander H. Reich [c], Shyam J. Deshpande [c], Geetanjali Kaushik [d], Arvind Chel [d], Julian D. Marshall [e,*], William W Nazaroff [f]

[a] Energy and Resources Group, University of California, Berkeley, CA 94720-3050, USA
[b] Environmental Energy Technologies Division, Lawrence Berkeley National Laboratory, Berkeley, CA 94720, USA
[c] Grinnell College, Grinnell, IA 50112-1670, USA
[d] Indian Institute of Technology Delhi, Hauz Khas, New Delhi 110016, India
[e] Department of Civil Engineering, University of Minnesota, 500 Pillsbury Drive SE, Minneapolis, MN 55455, USA
[f] Department of Civil and Environmental Engineering, University of California, Berkeley, CA 94720-1710, USA

ARTICLE INFO

Article history:
Received 15 February 2011
Received in revised form
7 May 2011
Accepted 9 May 2011

Keywords:
Particulate matter
Megacity
Microenvironment
Urban air quality
Transportation
Exposure

ABSTRACT

Concentrations of air pollutants from vehicles are elevated along roadways, indicating that human exposure in transportation microenvironments may not be adequately characterized by centrally located monitors. We report results from ~180 h of real-time measurements of fine particle and black carbon mass concentration ($PM_{2.5}$, BC) and ultrafine particle number concentration (PN) inside a common vehicle, the auto-rickshaw, in New Delhi, India. Measured exposure concentrations are much higher in this study (geometric mean for ~60 trip-averaged concentrations: 190 μg m^{-3} $PM_{2.5}$, 42 μg m^{-3} BC, 280 × 10^3 particles cm^{-3}; GSD ~1.3 for all three pollutants) than reported for transportation microenvironments in other megacities. In-vehicle concentrations exceeded simultaneously measured ambient levels by 1.5× for $PM_{2.5}$, 3.6× for BC, and 8.4× for PN. Short-duration peak concentrations (averaging time: 10 s), attributable to exhaust plumes of nearby vehicles, were greater than 300 μg m^{-3} for $PM_{2.5}$, 85 μg m^{-3} for BC, and 650 × 10^3 particles cm^{-3} for PN. The incremental increase of within-vehicle concentration above ambient levels—which we attribute to in- and near-roadway emission sources—accounted for 30%, 68% and 86% of time-averaged in-vehicle $PM_{2.5}$, BC and PN concentrations, respectively. Based on these results, we estimate that one's exposure during a daily commute by auto-rickshaw in Delhi is as least as large as full-day exposures experienced by urban residents of many high-income countries. This study illuminates an environmental health concern that may be common in many populous, low-income cities.

1. Introduction

New Delhi, India, is among the ten largest metropolitan areas worldwide, with an estimated year-2003 population of 18.6 million people (Forstall et al., 2009). Particulate air pollution has been a longstanding problem in Delhi. Ambient concentrations of $PM_{2.5}$ and PM_{10} (mass concentrations of airborne particles with aerodynamic diameters, d_p, less than 2.5 and 10 μm, respectively) are regularly among the highest in the world and frequently an order of magnitude larger than in US cities (Gurjar et al., 2008; Mage et al., 1996). Air quality management efforts in Delhi devote special attention to vehicle emissions. Many private and public transit vehicles have been converted to operate using compressed natural gas (CNG) fuel, and two-stroke vehicles are being phased out of use (Reynolds and Kandlikar, 2008). However, owing to rapid increases in private motor vehicle use, the Delhi transportation sector remains a large and growing source of air pollution in that metropolis (Narain et al., 2010).

Research from around the world indicates that particle concentrations in transportation microenvironments – on and near roadways and inside vehicles – often exceed nearby ambient levels. Therefore exposures of people while in transit and for those who live or work near roadways may not be well characterized by conventional air quality monitoring stations (Kaur et al., 2007). Short-term exposure to elevated in-vehicle particle concentrations has been associated with subclinical cardiovascular effects in healthy populations (Riediker et al., 2004; Jacobs et al., 2010), and might serve as a trigger of acute health effects (e.g., myocardial

* Corresponding author. Tel.: +1 612 625 2397; fax: +1 612 626 7750.
E-mail address: julian@umn.edu (J.D. Marshall).

1352-2310/$ – see front matter © 2011 Elsevier Ltd. All rights reserved.
doi:10.1016/j.atmosenv.2011.05.028

infarction) for susceptible individuals (Peters et al., 2004). Relatively few studies have investigated in-traffic exposures to particulate air pollution in developing-world megacities (Han and Naeher, 2006). Such exposures are of concern owing to high-emitting vehicle fleets, rapid increases in vehicle use, and long exposure durations in and near traffic. For example, a 1997 study in Delhi reported that concentrations of $PM_{5.0}$ and CO inside vehicles exceeded the high urban background concentrations by 1.5–10×, depending on vehicle type (Saksena et al., 2007).

In view of the limited data on this important air quality issue, we undertook an investigation of the ambient and in-vehicle concentrations in New Delhi of three constituents of vehicle exhaust: fine particles ($PM_{2.5}$), black carbon (BC), and ultrafine particle number (PN). Epidemiological evidence links $PM_{2.5}$ exposure to elevated risks for several acute and chronic health outcomes, including cardiovascular disease and premature mortality (Pope and Dockery, 2006; Brook et al., 2010). Black carbon – a product of incomplete combustion and a component of $PM_{2.5}$ – is associated with "probable" human carcinogens such as diesel exhaust (IARC, 1989) and polycyclic aromatic hydrocarbons (IARC, 1983). Particle number is typically dominated by ultrafine particles (UFP; diameter < 0.1 μm), which are abundant in vehicle exhaust (Kittelson, 1998) and are an emerging public health concern (Oberdörster, 2001; Delfino et al., 2005). To our knowledge, the research reported here constitutes the first published study that characterizes in-vehicle exposure concentrations to BC and PN on the Indian subcontinent. In addition, the measurements presented here represent one of the largest datasets for real-time, in-vehicle particle concentrations sampled anywhere.

2. Materials and methods

2.1. Site description and experimental design

New Delhi is India's capital and one of the country's more affluent cities. The region experiences cool winters (Dec–Jan); a brief, transitional spring (Feb–Mar); hot, dry summers (Apr–Jun); a hot, humid monsoon season (Jul–Sep); and a warm, dry post-monsoon season (Oct–Nov). Our study, conducted from February through May, spans the early spring through mid-summer period in Delhi. In this study, in-vehicle concentration measurements were collected primarily inside auto-rickshaws, a semi-enclosed, three-wheeled vehicle that offers little evident protection from exhaust plumes in outside air. Auto-rickshaws are ubiquitous in many South Asian cities, serving a function similar to a conventional taxi but at lower fares (Harding and Hussein, 2010; Tiwari, 2003). The ~55,000 auto-rickshaws in New Delhi, comprising ~1% of the vehicle fleet, handle ~4% of non-pedestrian person-trips. For comparison, there were ~5 million registered private vehicles in Delhi in 2008 (Harding and Hussein, 2010; Narain et al., 2010). During our measurement sessions, nearby traffic consisted of motorcycles, auto-rickshaws, light-duty passenger vehicles (LDV), three-wheeled cargo vehicles, small trucks, and buses. The most common fuels in use during this study were gasoline, diesel, and CNG. Heavy-duty trucks are prohibited from being driven in Delhi during daytime hours (6:00–21:00). Diesel-fueled cars comprise ~30% of the Delhi LDV fleet (Narain et al., 2010).

2.1.1. In-vehicle measurements

We measured in-vehicle concentrations on 40 weekdays (total sampling time ~180 h) during February 22 to May 26, 2010. Auto-rickshaw measurements (31 days, 62 trips, 160 h) were primarily conducted inside a single Bajaj model RE-4S TSR vehicle, the most common model in Delhi (Harding and Hussein, 2010). This open-sided vehicle holds 1–4 occupants in an interior volume of ~1 m^3, has a maximum speed of 50–60 km h^{-1}, and is powered by a 300 cm^3 displacement, 5–6 kW four-stroke compressed natural gas (CNG) engine. Instruments were carried inside the vehicle in a padded backpack designed to limit instrument tilt and vibration. We situated sampling lines for all instruments to measure at a typical breathing height for a passenger in the center of the rear passenger seat. Supplemental experiments suggest that self-pollution from the auto-rickshaw's own exhaust did not make a substantial contribution to in-vehicle concentrations either while stopped or when traveling. (See Online Supplemental Information (SI) for details.) Drivers and research staff were nonsmokers.

The sampling route (one-way length: 19.5 km, Fig. 1) was selected to reflect the range of traffic conditions typical of south and central Delhi. The route connects an upper-income neighborhood, Chittaranjan Park (CRP), with a central commercial district, Connaught Place (CP). The route passes through residential, commercial, and office districts and incorporates several road types, including

Fig. 1. Map of New Delhi indicating the main sampling route used in the study. Each trip was driven out-and-back once each during AM and PM commute hours from the ambient monitoring site (Chittaranjan Park, CRP) to central New Delhi. Trips turned back at Connaught Place (CP; point 1 on map) during Feb–April (total distance: 39 km) and at Shrimant Madhav Rao Scindia Marg (point 2 on map) during May (total distance: 37 km). Each trip stopped at Lodhi Garden park (LG) for 30 min of ambient measurements.

narrow residential streets, 2–4 lane arterial roads with traffic signals, and 6–8 lane arterial roads with flyover intersections. The route was driven round-trip twice per sampling day: once during morning (08:30–11:30) and once during evening commute times (17:45–20:45; total travel: 78 km d^{-1}). We stopped midway through the route to measure ambient pollutant concentrations for 30 min inside a large urban park (see next section). Drivers were instructed to drive as they normally would, which in Delhi involves frequently changing lanes to avoid stopped vehicles and to reach the front of the queue at signals. As is typical of many Indian cities, traffic speeds were low. The median trip-integrated arithmetic mean speed was 18 km h^{-1} (10% trimmed range: 15–20 km h^{-1}). In the final sampling month (May 2010, 9 trips), we shortened our route by 2 km (~5%) owing to terrorism concerns at CP; overall traffic speeds and trip duration remained similar for the shortened route.

In addition to the primary sampling program, we explored variability in exposure concentrations with vehicle type and ventilation setting, as follows. We measured concentrations at the driver's side rear seat of a common car model (Tata Indica) on 15 trips on the same route and times-of-day, May 17–26. We operated the car either with open windows (5 trips) or with minimal air intake (10 trips). During open-window (OW) trips, windows were lowered halfway and the ventilation system was off. During trips with minimal air intake (RC), windows were closed, air conditioning was active, and the ventilation system was set to recirculate air at medium fan speed.

2.1.2. Ambient air quality monitoring: Chittaranjan Park (CRP) and Lodhi Garden (LG)

We conducted routine ambient air measurements in the Chittaranjan Park (CRP) neighborhood and inside Lodhi Garden (LG) park. The start of the sampling route was located at CRP, in south Delhi. Air-quality monitoring was performed continuously at this location. Like other affluent neighborhoods in Delhi, CRP (area, $A = 1.1$ km^2, population density = 16,000 people km^{-2}) contains 3–5 story residential buildings and dense shade tree cover; vehicle traffic is largely restricted to a few main roads. Monitoring was conducted on a building rooftop (height 13 m) situated 200–250 m from the nearest roadway with continuous vehicle flow, and 1000 m from the nearest major arterial roadway. Instruments were housed in a 1-m^3 sampling enclosure with 24-h power supply via electricity with battery backup. Local sources of air pollution were only observed occasionally and included vehicle traffic, wood and leaf combustion for heating and cooking outdoors (e.g., by security guards), trash burning, and construction activity.

Measurements at LG ($A = 0.3$ km^2) occurred during a 15–20 min period midway through each morning and evening mobile monitoring session. There were no evident major emissions sources in the park and the sampling location (~1 m above ground) was more than 230 m from the nearest roadway.

2.2. Instrumentation

2.2.1. Meteorological parameters

We employed a weather station (Model PWS-1000TD, Zephyr Instruments, East Granby, CT) to record meteorological parameters at CRP. The instrument was situated 2 m above roof height (15 m above ground level). Temperature (T), relative humidity (RH), wind speed (WS) and direction, and precipitation were logged at 5-min intervals over the entire study duration (14 weeks). The study was conducted between early spring (February, mean daily temperature range 16–27 °C) and peak summer (April–May, 30–44 °C). The interquartile range (IQR) wind speed was 0.7–1.3 m s^{-1}, primarily from the NE. Little rainfall occurred during the study (<2 cm $month^{-1}$). Trip-averaged meteorological data are reported in Table 1.

2.2.2. Continuous and integrated $PM_{2.5}$ measurements

We measured $PM_{2.5}$ concentrations using two DustTrak aerosol monitors (model 8520, TSI, Inc., Shoreview, MN). This instrument uses a laser photometer to determine real-time PM mass concentration based on 90° light scattering (Arku et al., 2008). Instruments were fitted with manufacturer-supplied $PM_{2.5}$ inlet nozzles and impactors. Each day, internal pumps were adjusted to the specified 1.7 L min^{-1} flow rate. The instrument zero point was calibrated daily using an external HEPA filter. One DustTrak was continuously operated (except during maintenance) at the ambient sampling location (CRP) from February 16 to April 23. A second DustTrak was used for mobile sampling between February 16 and May 26 and for ambient measurements after April 23. A short length (<30 cm) of conductive tubing (6 mm in diameter) was used to minimize particle loss. The DustTrak's recording interval was 1 s at LG and in-vehicle, and 30 s at CRP.

The DustTrak's light-scattering measurement technique is subject to error because the amount of light scattered by particles depends on relative humidity and particle properties such as shape, size, and refractive index (Arku et al., 2008; Chakrabarti et al., 2004; Ramachandran et al., 2003). We applied two corrections to minimize error. First, we accounted for real-time effects of RH on instrument response using the approach of Ramachandran et al. (2003):

$$PM2.5_{RH-corrected} = \frac{PM2.5_{raw}}{CF},\quad CF = 1 + 0.25\frac{RH^2}{(1-RH)} \qquad (1)$$

Here, RH is the most recent 5-min average RH at CRP, expressed as a fraction of 100%. Although Eq. (1) is unstable for very high relative humidity ($RH \rightarrow 1$), the instantaneous relative humidity never exceeded 65% during our measurements. The trip-averaged RH correction factor (CF) was moderate during late February (mean: 1.17, maximum: 1.22) and small during other months (mean: 1.05, maximum: 1.15). Second, a mass-based calibration, derived from a comparison with $PM_{2.5}$ concentrations determined by gravimetric analysis of 32 colocated filter samples (concentration range: ~50–300 μg m^{-3}), was applied to the RH-corrected DustTrak measurements (see SI for details):

$$PM2.5_{gravimetric} = 3.91(PM2.5_{RH-corrected})^{0.706} \qquad (2)$$

Here, $PM2.5_{gravimetric}$ represents the estimated gravimetric-equivalent concentration, based on RH-corrected DustTrak measurements, and both mass concentration determinations have units of μg m^{-3}. For the 60 sampling trips with available data, the mean

Table 1
Monthly mean and range of meteorological parameters at the Chittaranjan Park (CRP) ambient site during morning (AM) and evening (PM) auto-rickshaw trips.

Month	Hours	Temperature (°C)		Relative humidity (%)		Wind speed (m s^{-1})	
(2010)	(trips)	AM	PM	AM	PM	AM	PM
Feb	23 (8)	26 (24–27)	23 (23–24)	52 (48–56)	56 (52–60)	0.9 (0.3–1.5)	0.2 (0.1–0.5)
Mar	62 (22)	33 (27–39)	30 (25–34)	35 (19–46)	37 (23–51)	0.6 (0.3–0.9)	0.3 (0.1–0.7)
Apr	48 (16)	41 (38–44)	37 (33–38)	16 (12–29)	21 (16–33)	0.5 (0.2–1.1)	<0.15
May	41 (16)	39 (34–43)	37 (28–40)	26 (12–48)	23 (13–52)	0.6 (0.3–1.1)	0.4 (0–1.1)

ratio of gravimetric-calibrated to *RH*-corrected $PM_{2.5}$ concentration was 0.74 for in-vehicle measurements and 0.91 for ambient measurements.

2.2.3. Black carbon measurements

We measured black carbon (BC) concentrations in-vehicle and at CRP using two portable aethalometers (model AE-51 "micro-Aeth," Magee Scientific, Berkeley, CA). These instruments report BC concentration at 1-s intervals by measuring changes in light attenuation ($\lambda = 880$ nm) on a disposable filter through which sample air is drawn at 100–150 $cm^3\ min^{-1}$.

Aethalometer measurements required substantial post-processing. The aethalometer frequently recorded spurious concentration "spikes" of ±200–2000 $\mu g\ m^{-3}$ BC when exposed to mild mechanical shock or vibration. As controlled testing of the instrument revealed a distinctive pattern for this spurious signal, we were able to remove nearly all occurrences of these spikes by developing and applying a custom post-processing algorithm to the 1 Hz raw signal from the instrument (see SI).

Previous laboratory and field experiments have revealed that the default aethalometer algorithm underestimates BC concentration as filter BC mass increases, especially when sampling highly light-absorbing particles (Jimenez et al., 2007; Kirchstetter, 2007; Kirchstetter and Novakov, 2007). We corrected for this effect using the empirical relationship of Kirchstetter and Novakov (2007), which was subsequently found in a study of heavy-duty diesel exhaust plumes (Ban-Weiss et al., 2009) to yield good agreement between thermal-optical analysis and aethalometer measurements of BC:

$$BC = BC_o(0.88Tr + 0.12)^{-1} \quad (3)$$

Here, *BC* is the corrected black carbon concentration, BC_o is the instrument-reported concentration, and $Tr = exp(-ATN/100)$ is the aethalometer filter transmission that is calculated from the instrument-reported attenuation coefficient (*ATN*). We applied Eq. (3) to all BC measurements. Trip-averaged correction factors (BC/BC_o) for in-vehicle BC measurements were greater than those for ambient measurements (medians: 1.58 in-vehicle, 1.23 ambient) owing to the more rapid filter loading experienced in on-road sampling conditions.

2.2.4. Ultrafine particle number concentration measurements

We measured ultrafine particle number concentrations (PN) using a portable condensation particle counter (CPC, model CPC 3007, TSI Inc., Shoreview, MN; frequency: 1 Hz). Although this instrument detects particles in the size range 10 nm $< d_p <$ 1 μm, PN is a reasonable proxy for UFP ($d_p < 0.1$ μm) under the conditions encountered in this study. Above the manufacturer-established concentration limit of 100,000 particles cm^{-3}, measurements are subject to undercounting because of particle coincidence errors (Knibbs et al., 2007; Westerdahl et al., 2005). To extend the effective maximum concentration limit of the instrument, we used an apparatus described by Ban-Weiss et al. (2009), which diluted the influent sample by ~5.5×. The device split the sample into two unequal paths: ~15% of flow passed through a 0.6 mm orifice (O'Keefe Controls, Trumbull, CT) and ~85% of flow passed through a HEPA filter. The flows were rejoined before entering the instrument. To ensure stable performance of the dilution system, we replaced the HEPA filter every 2–4 weeks and measured the dilution ratio daily. Over the life of each filter, measured dilution ratios were within 10–20% of the median value for that filter. For each filter used, we applied the median measured dilution ratio to all PN measurements made during the period of use of that filter (range: 5.39–5.95).

With the dilution system in place, concentrations still exceeded the 100,000 particles cm^{-3} threshold for 5% of measurements. We used the following equation to account for undercounting (Westerdahl et al., 2005) and dilution:

$$PN = PN_{diluted} \times DF,$$

$$PN_{diluted} = \begin{cases} 38456 \exp\left(PN_{raw} \times 10^{-5}\right), & PN_{raw} > 10^5 \\ PN_{raw}, & PN_{raw} \le 10^5 \end{cases} \quad (4)$$

Here, all PN parameters are in units of particles cm^{-3}; PN_{raw} represents instrument-measured PN; and *DF* is the dilution factor (whose average over all trips was ~5.5). Including this correction for readings above 100,000 particles cm^{-3} only slightly increased the overall trip-average PN concentrations (median increase: 3%; 10% trimmed range: 2–8% increase). As only one CPC was available, ambient PN levels reported here reflect the average of three mean concentrations: at LG mid-trip and at CRP for the 30-min periods immediately preceding and following each in-vehicle sampling period.

2.2.5. Other measurements and protocols

We used a handheld GPS receiver (model GPSMap 60CSx, Garmin, Inc., Olathe, KS) to record position (accuracy: ±3–5 m) and speed of the sampling vehicle at 1 Hz frequency. We synchronized instrument clocks daily. During each trip, we made a video recording of road conditions through the front window. We also manually recorded visual observations of local traffic conditions, high-emitting vehicles, and prominent non-vehicular emissions (e.g., roadside trash burning). We checked all instruments every 15 min to ensure proper operation. Malfunctioning instruments were restarted when possible.

2.3. Quality control, data processing and analysis

We downloaded, inspected, and archived real-time measurements immediately following each sampling session. Potential data quality issues (missing data, negative or otherwise spurious readings) were flagged for subsequent evaluation and resolution. We used custom software written in MATLAB (Mathworks, Inc., Natick, MA) to import, synchronize, and combine datasets and to apply corrections and calibrations. We censored a small number of records owing to instrument malfunction or substantial missing data. Fig. 2 presents illustrative data.

To ensure consistency between the paired instruments used to measure ambient and in-vehicle concentrations, we colocated both aethalometers and both DustTraks at CRP for the 30 min immediately before and after each sampling session. The DustTrak used for ambient measurements indicated a consistent bias of −7.3 ± 3.0 $\mu g\ m^{-3}$ $PM_{2.5}$ relative to the instrument used for in-vehicle measurements and gravimetric calibrations. To remove the mean bias, we adjusted the ambient instrument's measurements by +7.3 $\mu g\ m^{-3}$. Colocated measurements of BC agreed closely after applying the loading correction and spike-removing algorithm to the aethalometer data and so were not further adjusted (see SI).

For each session, microenvironment, and pollutant, we computed time-integrated arithmetic mean concentrations and concentration rank-percentiles for the 1-Hz series. When simultaneous in-vehicle and ambient measurement was not possible (PN; some days of $PM_{2.5}$ measurement), we imputed ambient levels as the arithmetic mean of the time-averaged values for the three short-duration ambient measurements: LG (mid-trip) and CRP (30 min before and after in-vehicle sampling). We validated this approach for the ~40 sessions in which simultaneous real-time ambient $PM_{2.5}$ and BC data were collected. The imputed and

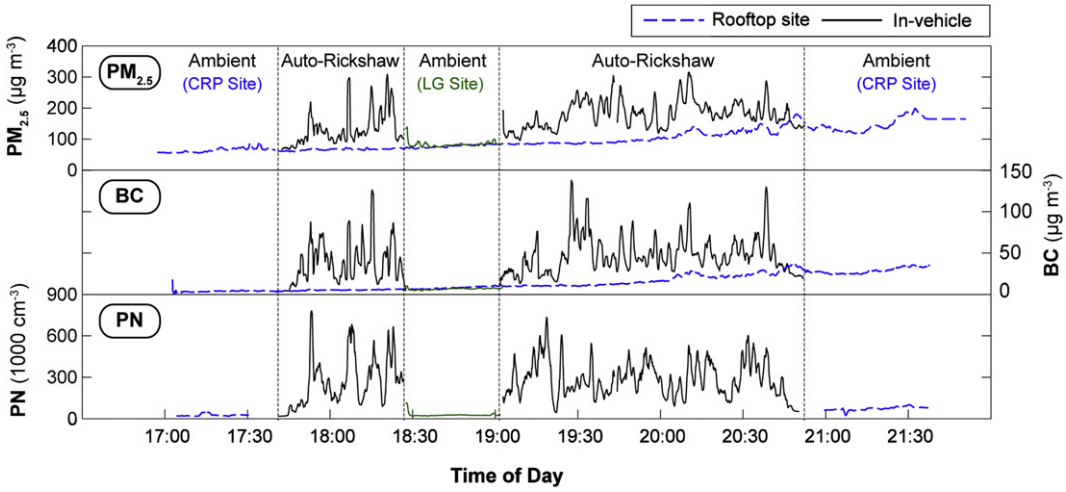

Fig. 2. Example data for one trip (29 March 2010, evening). For visual presentation, plotted concentrations were smoothed using a 60-s moving average filter.

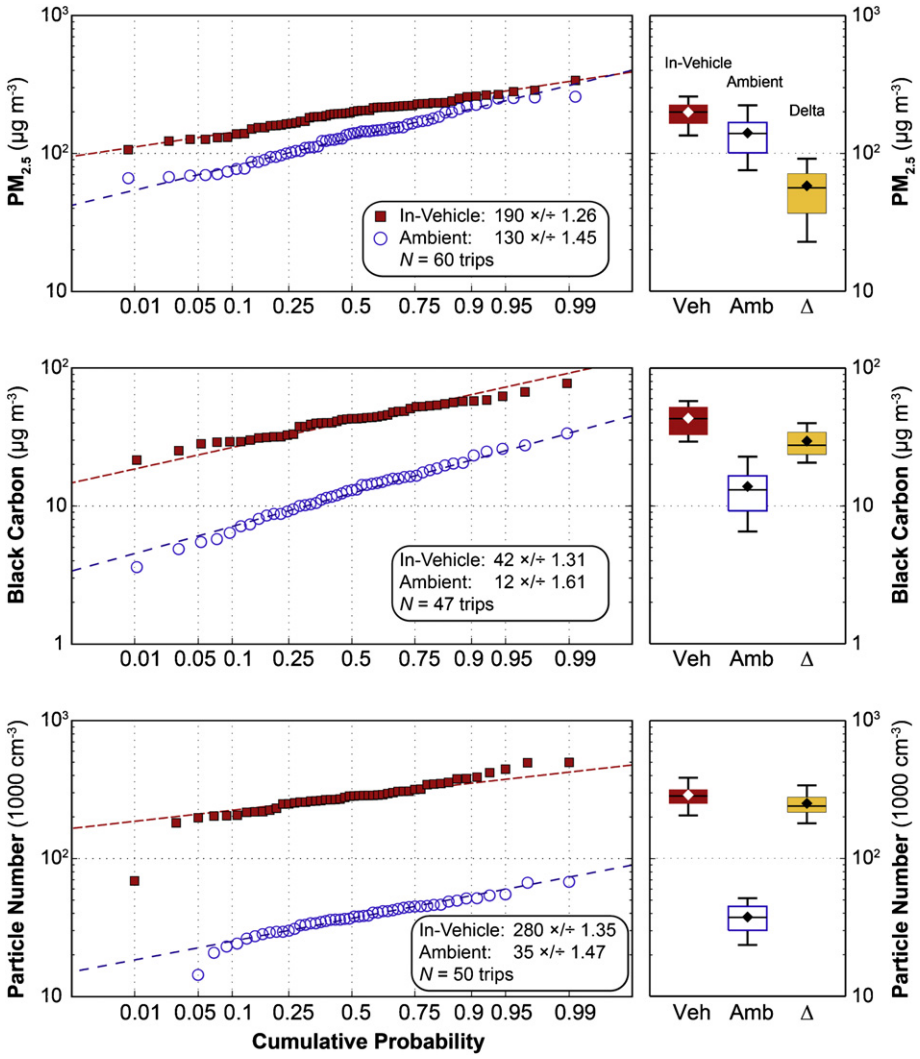

Fig. 3. Lognormal probability plots (left) and box plots (right) for trip-averaged auto-rickshaw concentrations. For left frames, lines indicate the best-fit lognormal distribution for each microenvironment and pollutant. Text boxes report geometric mean ×/÷ geometric standard deviation for each pollutant; *N* represents the number of valid, complete trips sampled for each pollutant. Here and elsewhere, box plots display the following distributional parameters: median (central horizontal line), mean (diamond), 25th and 75th percentiles (box), and 10th and 90th percentile (whiskers). Incremental in-vehicle concentrations (Δ, "delta") are calculated as the difference between the mean in-vehicle and ambient concentration during each trip.

Table 2
Distribution of average particulate matter concentrations for 62 auto-rickshaw trips in New Delhi.[a]

Pollutant	Location	AM (SD)	GM (GSD)	Median	Min	P_{10}	P_{25}	P_{75}	P_{90}	Max
$PM_{2.5}$ ($\mu g\ m^{-3}$)	Auto-Rickshaw	200 (46)	190 (1.27)	200	110	130	160	230	260	340
$N = 60$	Ambient	140 (52)	130 (1.45)	140	66	75	100	170	220	260
	Difference	58 (31)	47 (2.50)	56	0	23	37	72	91	160
BC ($\mu g\ m^{-3}$)	Auto-Rickshaw	43 (12)	42 (1.31)	43	22	29	33	52	58	77
$N = 47$	Ambient	14 (6.3)	12 (1.61)	13	3.6	6.5	9.2	17	23	34
	Difference	29 (9.0)	28 (1.36)	27	10	21	24	34	40	63
PN ($10^3\ cm^{-3}$)	Auto-Rickshaw	290 (77)	280 (1.35)	280	69	200	250	320	380	500
$N = 50$	Ambient	38 (12)	35 (1.47)	37	9.8	24	30	45	51	68
	Difference	250 (72)	240 (1.41)	240	45	180	220	280	340	460

[a] "Difference" represents the trip-average concentration in the the auto-rickshaw microenvironment minus the concentration determined for the ambient site at Chittaranjan Park (CRP). Abbreviations: AM – arithmetic mean, SD – arithmetic standard deviation, GM – geometric mean, GSD – geometric standard deviation, P_{10}, P_{25}, P_{75}, and P_{90} – 10th, 25th, 75th, and 90th percentiles of distribution of trip-average concentrations.

actual mean concentrations agree well (median bias <5%, Pearson's r^2 of 0.89 for $PM_{2.5}$ and 0.85 for BC). As only a single CPC was available, we were not able to directly validate this approach for PN. Quality control and data processing reduced the concentration dataset from $\sim 2 \times 10^6$ observations to, respectively, 60, 47 and 50 matched pairs of arithmetic mean in-vehicle and ambient $PM_{2.5}$, BC, and PN collected on a total of 62 trips.

3. Results and discussion

3.1. In-vehicle concentrations: auto-rickshaws

Particle concentrations measured in auto-rickshaws were high. Trip-averaged concentrations were approximately lognormally distributed (Fig. 3), with geometric means of 190 $\mu g\ m^{-3}$ for $PM_{2.5}$, 42 $\mu g\ m^{-3}$ for BC, and 280×10^3 particles cm^{-3} for PN (Table 2). Concentrations were elevated in-vehicle relative to ambient measurements at CRP, which had geometric means of 130 $\mu g\ m^{-3}$ for $PM_{2.5}$, 12 $\mu g\ m^{-3}$ for BC, and 35×10^3 particles cm^{-3} for PN. Over all trips, the arithmetic mean incremental in-vehicle (auto-rickshaw minus ambient) concentration was $58 \pm 8.0\ \mu g\ m^{-3}$ for $PM_{2.5}$, $29 \pm 2.6\ \mu g\ m^{-3}$ for BC, and $(250 \pm 20) \times 10^3$ particles cm^{-3} for PN (mean ± 95% CI). For context, note that annual average $PM_{2.5}$ among all ambient monitors in the US (sites predominantly urban) was 11 $\mu g\ m^{-3}$ during 2006–2008 (US EPA, 2008).

We observed frequent short-duration (~10–100 s) concentration peaks for all monitored pollutants. The 95th percentile of 10-s averaged concentrations exceeded the trip arithmetic mean concentration by ~1.5–2.3× (Table 3). Video data suggest that many transient high concentrations ($PM_{2.5} > 500\ \mu g\ m^{-3}$, BC > 400 $\mu g\ m^{-3}$, PN > 10^6 particles cm^{-3}) may be attributable to visibly high-emitting vehicles, a finding that is consistent with recent laboratory emissions tests of New Delhi auto-rickshaws linking visible plumes with high $PM_{2.5}$ emissions (Reynolds et al., 2011).

Concentrations of the individual pollutants were only weakly correlated with each other: Pearson's r^2 for $PM_{2.5}$–BC, $PM_{2.5}$–PN, and BC–PN, respectively were 0.11, 0.28, and 0.08 for trip-average concentrations, and 0.33, 0.10, and 0.12 for 1-min average pollutant concentrations during trips (mean over all trips). Correlations between in-vehicle and ambient concentrations were also only moderate: Pearson's r^2 for trip-average concentrations were 0.65 ($PM_{2.5}$), 0.42 (BC), and 0.31 (PN).

3.2. Contribution of proximate sources to in-vehicle exposure concentrations

To the extent that in-vehicle concentrations differ systematically from ambient concentrations, ambient air quality measurements may not adequately represent in-traffic exposures. The in-vehicle to ambient concentration ratio (γ) is a metric that can usefully characterize this difference. In theory, this ratio will be greater for pollutants that are predominantly emitted on roadways. Furthermore, among those pollutants emitted primarily on roadways, the ratio will be higher for nonconserved pollutants that decay on time scales that are as fast or faster than the air transit time from emission site to ambient receptor. A review of 25 studies reported that a typical value of γ for primary, vehicle-derived conserved pollutants is ~4:1 (Marshall et al., 2003). For each of the pollutants measured in this study, we computed the distribution of γ over all trips (Table 3). For BC – a primary, conserved pollutant and a marker for vehicle emissions – we found arithmetic mean $\gamma = 3.6$ (95% CI: 3.1–4.1), comparable to the value reported by Marshall et al. We obtained a lower mean value for $PM_{2.5}$, $\gamma = 1.5$ (95% CI: 1.4–1.6). That this result is less than for BC is not surprising because $PM_{2.5}$ is a conserved, regional pollutant (i.e., not a tracer for

Table 3
Summary statistics for within-trip concentration distributions inside auto-rickshaws. [a]

Pollutant	Auto-Rickshaw Concentrations			Ratio Mean Auto: Mean Ambient (γ)	Ratio P_{95} Auto: Mean Auto	Ratio P_{95} Auto: Mean Ambient
	P_5	P_{95}	Max			
	GM (GSD)	GM (GSD)	GM (GSD)	AM	AM	AM
$PM_{2.5}$ ($\mu g\ m^{-3}$)	110 (1.4)	300 (1.2)	690 (1.4)	1.5	1.5	2.4
BC ($\mu g\ m^{-3}$)	12 (1.5)	88 (1.3)	400 (2.1)	3.6	2.1	7.8
PN ($10^3\ cm^{-3}$)	53 (1.4)	650 (1.4)	1600 (1.6)	8.4	2.3	20

[a] "P_5" and "P_{95}" indicate, respectively, the 5th and 95th percentile 10-s averaged concentration measurement for a given commute trip; Max indicates the maximum 10-s averaged concentration measurement for that trip. Measures of central tendency (AM = arithmetic mean, GM = geometric mean) and of spread (GSD = geometric standard deviation) are for the distribution of values over all 47–60 trips with available data. Concentration ratios were computed for each individual trip; the value reported here is the AM of the distribution of ratios over all trips. See text for description of γ, the ratio of trip-averaged in-vehicle to ambient concentration.

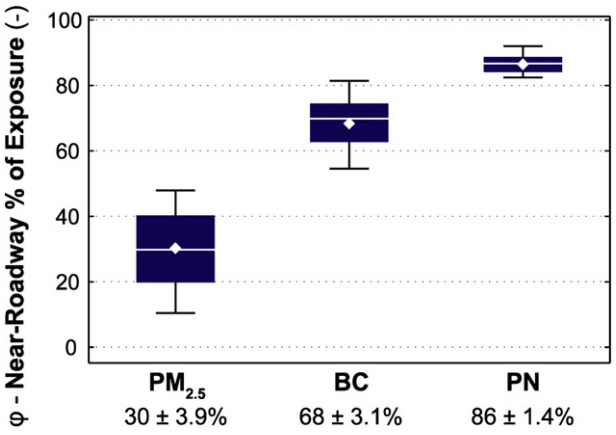

Fig. 4. Box plots of trip-averaged in-vehicle concentration attributable to near-roadway microenvironment (φ, see text). Numbers indicate mean ± 95% confidence interval.

vehicle emissions); thus in-vehicle concentrations are only moderately elevated above the high background levels. Receptor modeling for Delhi conducted in 2001 suggests that road dust and vehicle emissions each account for only ~20–25% of ambient $PM_{2.5}$ during the spring (Chowdhury et al., 2007). The value γ =1.5 reported here for $PM_{2.5}$ in Delhi is consistent with the value of 1.4 reported by Both et al. (in press) for mid-day $PM_{2.5}$ concentrations on-road versus on a residential roof in a low-income neighbourhood in Bangalore, India. Interestingly, for PN, we found a higher mean value, $\gamma = 8.4$ (95% CI: 7.3–9.6). This finding, too, is qualitatively consistent with expectations. PN, a strong marker for vehicle exhaust plumes, is a nonconserved pollutant. Coagulation, evaporation, and deposition onto surfaces can remove ultrafine particles at time scales that compete with the residence time of air in urban areas. (For advection across New Delhi, at a scale of 40–50 km with wind speeds of 1–2 m s^{-1}, the time scale is ~5–10 h.) Mönkkönen et al. (2004) observed evidence of a strong coagulation sink for UFP in New Delhi. We estimate a time scale of ~0.3–3 h for coagulation of 10–100 nm particles for ambient conditions in New Delhi (see SI).

We infer the contribution of roadway emissions to in-vehicle exposures by computing the difference between mean in-vehicle and ambient (CRP) concentrations for each of the 62 trips. We estimate the fraction of the in-vehicle concentration attributable to the roadway microenvironment (φ) as

$$\varphi = (C_{veh} - C_{amb})/C_{veh} = 1 - \gamma^{-1} \quad (5)$$

Here, for a given sampling session, C_{veh} is the mean in-vehicle concentration and C_{amb} is the mean ambient concentration at CRP. As illustrated in Fig. 4, φ was smallest for $PM_{2.5}$ (mean ± 95% CI: 30 ± 4%), intermediate for BC (68 ± 3%) and greatest for PN (86 ± 1%). The values of this metric indicate that in-vehicle concentrations of BC and PN are dominated by local (near and on-roadway) emissions.

As noted above, BC and UFP (and thus PN) are more specific markers of vehicle emissions than is $PM_{2.5}$. The ratio of concentrations for these two pollutants to $PM_{2.5}$ is an indicator of the extent to which microenvironmental concentrations are influenced by vehicle emissions. Over all trips, the mean ratio of BC:$PM_{2.5}$ was twice as high in the auto-rickshaw cabin as it was at the ambient site (in-vehicle BC:$PM_{2.5}$ = 0.23; ambient BC:$PM_{2.5}$ = 0.10). The ratio of PN:$PM_{2.5}$ was ~5× higher inside the auto-rickshaw cabin than for ambient measurements (in-vehicle PN:$PM_{2.5}$: 1.4 × 10^9 particles μg^{-1}; ambient PN:$PM_{2.5}$: 0.3 × 10^9 particles μg^{-1}).

3.3. Seasonal and temporal variability in ambient and in-vehicle pollutant concentrations

We used unbalanced two-way analysis of variance (ANOVA) to decompose the variability in ambient and in-vehicle

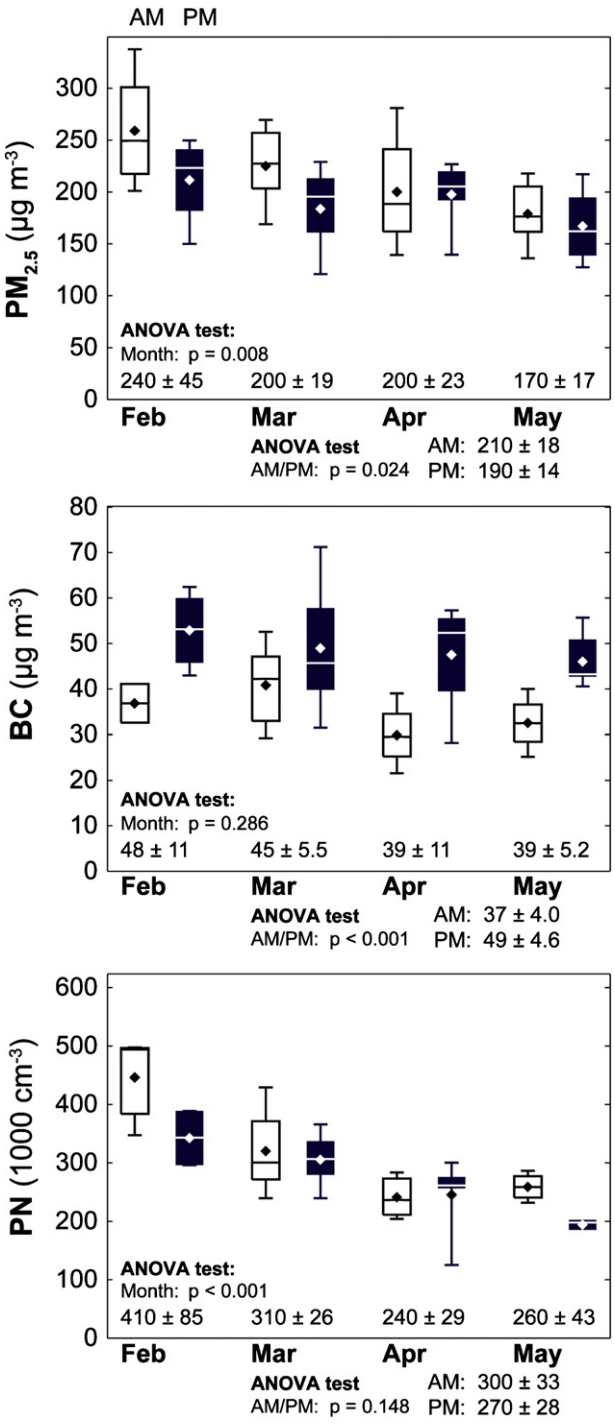

Fig. 5. Decomposition of variability in auto-rickshaw exposure concentrations into month-of-year and time-of-day components. Box plots indicate the distribution of in-vehicle concentrations for morning and evening trip samples during each month of the field campaign. Arithmetic mean ± 95% CI concentrations are indicated for each month (inside frames) and separately by morning and evening trip (below frames). *P*-values represent the result of unbalanced two-factor ANOVA test for effect of month and time-of-day on total concentration variability.

concentrations into time-of-day (AM vs. PM), day-of-week, and seasonal (month) components (Fig. 5, Fig. SI.5). We found statistically significant ($p < 0.05$) in-vehicle time-of-day trends for $PM_{2.5}$ and BC, but not for PN. On average, $PM_{2.5}$ and BC concentrations were, respectively, 11% higher and 32% lower in the morning as compared with the evening commutes. The reasons for the different behavior among the three species are not known. One plausible explanation derives from recognizing that in-vehicle concentrations are dependent on contributions from both the urban background and the near-vehicle microenvironment. The timing of in-vehicle $PM_{2.5}$ is dominated by the contribution from the urban background, whereas the temporal trend for BC appears to be attributable to the on-road microenvironment (Fig. SI.5). The increment for in-vehicle concentrations above the ambient levels was typically greater in the evening than in morning for both $PM_{2.5}$ and BC, which may reflect influences from temporal patterns of emissions and/or atmospheric transport and dispersion. We observed, for example, that wind speeds at the CRP ambient site were ~60% lower in the evening than in the morning (Table 1), a characteristic that would be consistent with relatively higher contributions of vehicle emissions to on-roadway concentrations during the evening commutes. Based on tests using ANOVA by day of week and multi-factorial ANOVA by day of week, time of day, and month, we did not detect any consistent day-of-week differences in concentration. Sampling was limited to Monday through Friday, so any weekend effects would not have been detected.

We found a statistically significant downward trend for in-vehicle $PM_{2.5}$ and PN concentrations between February and May. For $PM_{2.5}$, the seasonal concentration decrease was similar for in-vehicle and ambient conditions (Fig. SI.5), suggesting that urban-scale trends (e.g., fuel use for heating, average mixing height) are responsible for observed seasonal changes for in-vehicle concentrations. In contrast, seasonal decreases for PN were noticeably larger for in-vehicle than for ambient conditions. We hypothesize that changes in temperatures may explain this in-vehicle/ambient PN difference, owing to shifts in gas-particle partitioning of semi-volatile UFP constituents and the CPC's 10-nm particle size cut-point. Specifically, particles that would have been larger than 10 nm at lower temperatures might shrink via evaporation to diameters smaller than 10 nm at higher temperatures. The proportion of particles that are small (~10 nm) is expected to be higher near-source (on-roadway air, with fresh emissions) than in ambient air (more aged aerosols).

3.4. Comparisons among vehicle types

We examined differences by vehicle type for the trip-average concentration inside auto-rickshaws, cars with open windows (OW; no fan ventilation), and cars with ventilation set to recirculate air (RC; windows closed and air conditioning on) in May (Fig. 6a). We found no statistically significant difference between concentrations in auto-rickshaws and OW cars. However, concentrations were substantially lower inside RC cars than in the auto-rickshaw, with mean ± 95% CI concentration difference of 61 ± 33 μg m^{-3} for $PM_{2.5}$, 12 ± 11 μg m^{-3} for BC, and 130 ± 41 × 10^3 particles cm^{-3} for PN. Concentration ratios (RC car: auto-rickshaw) were ~0.6 for

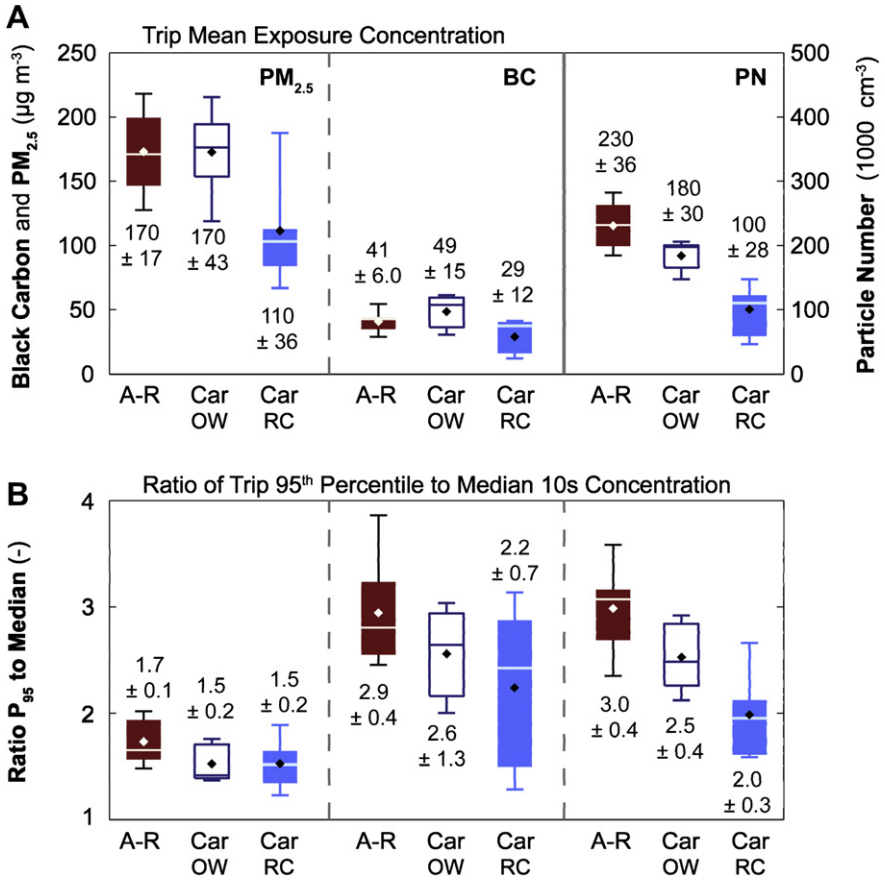

Fig. 6. Box plots of $PM_{2.5}$, BC, and PN in-vehicle exposure concentrations sampled in May 2010, by vehicle type, showing (A) concentrations and (B) a measure of skew (ratio of each trip's 95th percentile [P_{95}] to median concentration based on 10-s averages of concentration). Vehicle types: A–R, auto rickshaw; Car OW, Tata Indica with windows open; Car RC, Tata Indica with windows closed, air conditioning on, and ventilation set to recirculate air. Left axis indicates $PM_{2.5}$ and BC concentrations; right axis indicates PN concentration. Text displays arithmetic mean ± 95% CI. Total number of trips: auto-rickshaw (16), OW car (5), RC car (10).

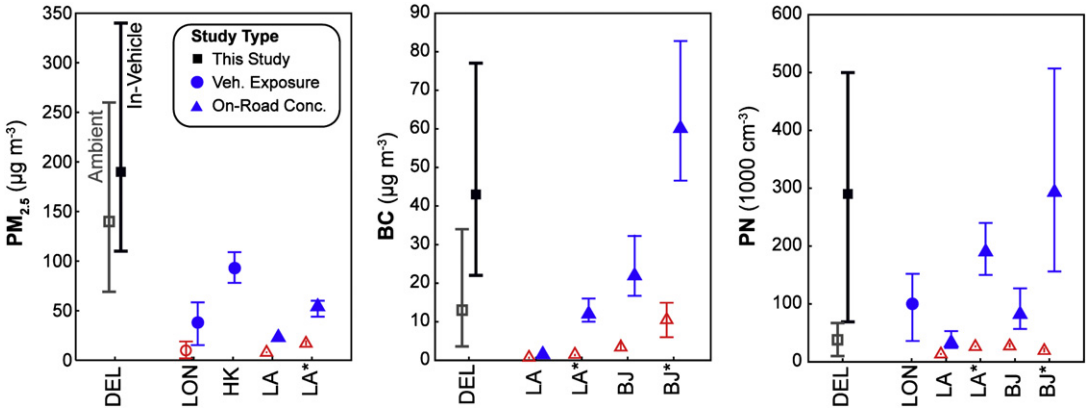

Fig. 7. Comparison of in-vehicle (solid) and ambient (open) concentrations from this study (Delhi, DEL) and from other megacities. Whisker plots indicate means and range of observations. In-vehicle studies were for cars (London, LON; Kaur et al., 2005) and non-AC buses (Hong Kong, HK; Chan et al., 2002). Mobile on-road measurements were for Los Angeles (LA; Fruin et al., 2008) and Beijing (BJ; Westerdahl et al., 2009). Extreme conditions in these cities are plotted as LA* (freeway with extensive heavy-duty truck traffic) and BJ* (truck dominated night traffic).

$PM_{2.5}$, 0.7 for BC and 0.4 for PN. Relative to auto-rickshaw concentrations, the range of instantaneous in-vehicle concentrations (Fig. 6b) was reduced for OW cars, and more substantially reduced for RC cars, as would be expected given the reduced air exchange rates for such vehicles (Ott et al., 2008; Fruin et al., 2011). If the auto-rickshaw PN exposure concentration measurements are similar to outdoor on-road levels, then the in-vehicle to outdoor PN ratio for the RC cars tested here (~0.4) is within the range (~0.2–0.6) reported in a previous US study (Zhu et al., 2007). To the extent that concentrations in auto-rickshaws reflect on-road levels, then travelers using other unenclosed transport modes (such as motorcycles, which account for ~20% of total trips in Delhi) may also experience trip-averaged exposures of similarly high magnitude. Further research is warranted to investigate exposures for unenclosed transport modes with driving patterns distinct from those of auto-rickshaws.

3.5. Comparison to other megacities, and implications for time-integrated exposure

In-vehicle concentrations reported here are ~2–10× greater than in-vehicle and on-road concentrations previously reported for other megacities (London, Los Angeles, Beijing, Hong Kong; see Fig. 7 and SI). Mean BC exposure concentrations in Delhi auto-rickshaws were roughly twice those measured on Beijing roads during the daytime and ~3–30× greater than those measured on Los Angeles arterial roadways and freeways with varying levels of diesel heavy-duty vehicle (HDV) traffic (Fruin et al., 2008; Westerdahl et al., 2005, 2009). Although few HDV were in use during our measurements, the BC levels in Delhi are higher than reported elsewhere. This finding might indicate that LDV in Delhi are high-emitters of BC, perhaps because of the substantial (~30%) and growing market share of diesel LDV in India (Narain et al., 2010).

A global review of 47 studies of commuter exposure to UFP reported geometric mean PN ~ 5–8× lower than measured in Delhi auto-rickshaws, depending on transport mode (Knibbs et al., 2011). However, there have been few prior investigations of in-vehicle exposure to PN in developing-world megacities. Auto-rickshaw PN exposure concentrations were 3× higher in Delhi than measured on Beijing roads during the daytime and comparable to levels measured there during diesel HDV-dominated nighttime traffic (Westerdahl et al., 2009). Moreover, the Delhi measurements were largely conducted during time periods of strong vertical mixing (daytime, high mixing height), likely in contrast with the nighttime measurements in Beijing. As has been observed by others, ambient PN levels are remarkably similar for New Delhi, Beijing, and Los Angeles, despite substantial diversity in demographics, source types, and emissions among these cities (Laakso et al., 2006). This observation may be influenced by the high mass concentration providing an effective coagulation sink for UFP under more highly polluted conditions. Finally, we note that the instruments used in this study may underreport total PN relative to the instruments used in other studies because of differences in the minimum size cutpoint (10 nm here, versus 3–7 nm in some other studies (Table SI.3)).

High in-vehicle concentrations in Delhi would lead to high time-integrated exposures. For example, a typical time-integrated exposure during an average daily commute (1.9 h d^{-1} for auto-rickshaw users (Saksena et al., 2007)) is ~530 × 10^3 particles cm^{-3} h d^{-1}, which is larger than any of (a) estimates for entire-day PN exposures for urban California residents (~330 × 10^3 particles cm^{-3} h d^{-1}; Fruin et al., 2008), (b) the average in-home exposure contributions for residents of seven San Francisco Bay Area single-family homes (~300 × 10^3 particles cm^{-3} h d^{-1}, Bhangar et al., 2011), and (c) the average for occupants of Beijing high-rise apartments (~290 × 10^3 particles cm^{-3} h d^{-1}, Mullen et al., in press). During a typical daily work shift (10–16 h; Harding and Hussein, 2010), auto-rickshaw drivers may receive very high PN exposures, on the order of (3000–4000) × 10^3 particles cm^{-3} h d^{-1}.

4. Conclusions

We measured in-vehicle exposure concentrations to particulate air pollution for auto-rickshaw and car commuters during three months in New Delhi, India. This paper reports one of the first sets of PN and BC exposure concentration measurements inside auto-rickshaws, a ubiquitous transport mode in South Asian urban areas. It also represents one of the longest-duration measurement campaigns of real-time, in-vehicle PN and BC concentrations anywhere. Auto-rickshaw exposure concentrations of $PM_{2.5}$, BC, and PN were very high in comparison with in-vehicle concentrations measured in other cities around the world. Short-duration trips by auto-rickshaw in New Delhi result in time-integrated exposures to particulate air pollution comparable to or greater than full-day exposures that would be experienced by residents of many urban areas in high-income countries.

Auto-rickshaw exposure concentrations were ~1.5× to 8× larger than, and only moderately correlated with, levels measured

at an urban background site. Correspondence between ambient and in-vehicle measurements was greatest for $PM_{2.5}$, probably because of the high regional background from secondary $PM_{2.5}$. In contrast, in-vehicle BC and PN exposures were predominantly attributable to in- and near-roadway sources. These results reinforce previously published findings that ambient monitoring often provides a poor proxy for in-vehicle exposures to vehicle-emitted pollutants.

Over the past decade, Delhi has made strong steps towards reducing vehicle emissions of PM, especially with the conversion of much of the city's bus fleet from diesel to CNG fuel (Reynolds and Kandlikar, 2008). Despite these efforts, $PM_{2.5}$, BC, and PN concentrations in Delhi's auto-rickshaws are among the highest values reported in the literature for routine exposures in transportation microenvironments. These measurements in auto-rickshaws may be representative of other open-window or unenclosed vehicles in Delhi, India. Three current trends suggest that the public health risks that are likely to be associated with these high exposures may persist and even worsen in the future. First, vehicle ownership and use are growing rapidly in Delhi and other Indian cities. Second, diesel LDVs are increasingly popular in India. Without effective emission controls, a trend toward increasing diesel LDV use is likely to be accompanied by increasing on-road BC emissions and concentrations. Third, increased adoption of CNG may reduce $PM_{2.5}$ emissions from spark-ignition engines, but at the cost of higher PN emissions (Mönkkönen et al., 2005). We suggest that further study of exposure to particulate air pollution is warranted in other populous South Asian cities, which have different vehicle fleets (older vehicles, more heavy-duty vehicles and two wheelers) and different fuel mixes (less CNG, more diesel and gasoline) in comparison to New Delhi.

Acknowledgments

The authors thank A. Sagar and G. Tiwari for hosting one of us (JSA) at the Indian Institute of Technology, Delhi during field research. We thank M. Apte, J. Blair, M. Brauer, A. Grieshop, L. Gundel, S. Guttikunda, O. Hadley, T. Hansen, M. Lunden, C. Reynolds, and K. Smith for technical assistance and feedback. In addition, we gratefully acknowledge the efforts of our research assistant Phoolchand. Efforts by JSA were partially supported by a Fulbright-Nehru grant from the US-India Educational Foundation and by the US Environmental Protection Agency under the EPA STAR Graduate Fellowship Program. The funding agencies neither reject nor endorse the conclusions and the views expressed herein.

Appendix. Supplementary material

Supplementary data associated with this article can be found, in the online version, at doi:10.1016/j.atmosenv.2011.05.028.

References

Arku, R.E., Vallarino, J., Dionisio, K.L., Willis, R., Choi, H., Wilson, J.G., Hemphill, C., Agyei-Mensah, S., Spengler, J.D., Ezzati, M., 2008. Characterizing air pollution in two low-income neighborhoods in Accra, Ghana. Science of the Total Environment 402, 217–231.

Ban-Weiss, G.A., Lunden, M.M., Kirchstetter, T.W., Harley, R.A., 2009. Measurement of black carbon and particle number emission factors from individual heavy-duty trucks. Environmental Science & Technology 43, 1419–1424.

Bhangar, S., Mullen, N.A., Hering, S.V., Kreisberg, N.M., Nazaroff, W.W., 2011. Ultrafine particle concentrations and exposures in seven residences in northern California. Indoor Air 21, 132–144.

Both, A.F., Balakrishnan, A., Joseph, B., Marshall, J.D. Spatiotemporal aspects of real-time $PM_{2.5}$: low- and middle-income neighborhoods in Bangalore, India. Environmental Science & Technology, in press doi: 10.1021/es104331w.

Brook, R.D., Rajagopalan, S., Pope III, C.A., Brook, J.R., Bhatnagar, A., Diez-Roux, A.V., Holguin, F., Hong, Y., Luepker, R.V., Mittleman, M.A., Peters, A., Siscovick, D., Smith Jr., S.C., Whitsel, L., Kaufman, J.D., 2010. Particulate matter air pollution and cardiovascular disease: an update to the scientific statement from the American Heart Association. Circulation 121, 2331–2378.

Chakrabarti, B., Fine, P.M., Delfino, R., Sioutas, C., 2004. Performance evaluation of the active-flow personal DataRAM $PM_{2.5}$ mass monitor (Thermo Anderson pDR-1200) designed for continuous personal exposure measurements. Atmospheric Environment 38, 3329–3340.

Chan, L.Y., Lau, W.L., Lee, S.C., Chan, C.Y., 2002. Commuter exposure to particulate matter in public transportation modes in Hong Kong. Atmospheric Environment 36, 3363–3373.

Chowdhury, Z., Zheng, M., Schauer, J.J., Sheesley, R.J., Salmon, L.G., Cass, G.R., Russell, A.G., 2007. Speciation of ambient fine organic carbon particles and source apportionment of $PM_{2.5}$ in Indian cities. Journal of Geophysical Research 112, D15303.

Delfino, R.J., Sioutas, C., Malik, S., 2005. Potential role of ultrafine particles in associations between airborne particle mass and cardiovascular health. Environmental Health Perspectives 113, 934–946.

Forstall, R.L., Greene, R.P., Pick, J.B., 2009. Which are the largest? Why lists of major urban areas vary so greatly. Tijdschrift voor economische en sociale geografie 100, 277–297.

Fruin, S., Westerdahl, D., Sax, T., Sioutas, C., Fine, P.M., 2008. Measurements and predictors of on-road ultrafine particle concentrations and associated pollutants in Los Angeles. Atmospheric Environment 42, 207–219.

Fruin, S.A., Hudda, N., Sioutas, C., Delfino, R.J., 2011. Predictive model for vehicle air exchange rates based on a large, representative sample. Environmental Science & Technology 45, 3569–3575.

Gurjar, B.R., Butler, T.M., Lawrence, M.G., Lelieveld, J., 2008. Evaluation of emissions and air quality in megacities. Atmospheric Environment 42, 1593–1606.

Han, X., Naeher, L.P., 2006. A review of traffic-related air pollution exposure assessment studies in the developing world. Environment International 32, 106–120.

Harding, S., Hussein, A., 2010. On the Road to Nowhere? Auto-rickshaws in Delhi: The System, Problems and Recommendations, Informal Labour Portfolio. AMAN Public Charitable Trust, New Delhi. Accessed at: http://www.amanpanchayat.org/documents/reports/simon-auto-final.doc.

IARC, 1983. Polynuclear Aromatic Compounds, Part 1, Chemical, Environmental and Experimental Data, vol. 32. International Agency for Research on Cancer (IARC) Monographs on the Evaluation of Carcinogenic Risks to Humans. Accessed at: http://monographs.iarc.fr/ENG/Monographs/vol32/volume32.pdf.

IARC, 1989. Diesel and Gasoline Engine Exhausts and Some Nitroarenes, vol. 46. International Agency for Research on Cancer (IARC) Monographs on the Evaluation of Carcinogenic Risks to Humans. Accessed at: http://monographs.iarc.fr/ENG/Monographs/vol46/volume46.pdf.

Jacobs, L., Nawrot, T.S., de Geus, B., Meeusen, R., Degraeuwe, B., Bernard, A., Sughis, M., Nemery, B., Int Panis, L., 2010. Subclinical responses in healthy cyclists briefly exposed to traffic-related air pollution: an intervention study. Environmental Health 9 Art. 64.

Jimenez, J., Claiborn, C., Larson, T., Gould, T., Kirchstetter, T.W., Gundel, L., 2007. Loading effect correction for real-time aethalometer measurements of fresh diesel soot. Journal of the Air & Waste Management Association 57, 868–873.

Kaur, S., Nieuwenhuijsen, M., Colvile, R., 2005. Personal exposure of street canyon intersection users to $PM_{2.5}$, ultrafine particle counts and carbon monoxide in Central London, UK. Atmospheric Environment 39, 3629–3641.

Kaur, S., Nieuwenhuijsen, M.J., Colvile, R.N., 2007. Fine particulate matter and carbon monoxide exposure concentrations in urban street transport microenvironments. Atmospheric Environment 41, 4781–4810.

Kirchstetter, T.W., 2007. Evaluating Past and Improving Present and Future Measurements of Black Carbon Particles in the Atmosphere. California Energy Commission, PIER Energy-Related Environmental Research. CEC-500-2007-042.

Kirchstetter, T.W., Novakov, T., 2007. Controlled generation of black carbon particles from a diffusion flame and applications in evaluating black carbon measurement methods. Atmospheric Environment 41, 1874–1888.

Kittelson, D.B., 1998. Engines and nanoparticles: a review. Journal of Aerosol Science 29, 575–588.

Knibbs, L.D., de Dear, R.J., Morawska, L., Coote, P.M., 2007. A simple and inexpensive dilution system for the TSI 3007 condensation particle counter. Atmospheric Environment 41, 4553–4557.

Knibbs, L.D., Cole-Hunter, T., Morawska, L., 2011. A review of commuter exposure to ultrafine particles and its health effects. Atmospheric Environment 45, 2611–2622.

Laakso, L., Koponen, I.K., Mönkkönen, P., Kulmala, M., Kerminen, V.-M., Wehner, B., Wiedensohler, A., Wu, Z., Hu, M., 2006. Aerosol particles in the developing world; a comparison between New Delhi in India and Beijing in China. Water, Air, and Soil Pollution 173, 5–20.

Mage, D., Ozolins, G., Peterson, P., Webster, A., Orthofer, R., Vandeweerd, V., Gwynne, M., 1996. Urban air pollution in megacities of the world. Atmospheric Environment 30, 681–686.

Marshall, J.D., Riley, W.J., McKone, T.E., Nazaroff, W.W., 2003. Intake fraction of primary pollutants: motor vehicle emissions in the South Coast Air Basin. Atmospheric Environment 37, 3455–3468.

Mönkkönen, P., Koponen, I.K., Lehtinen, K.E.J., Hämeri, K., Uma, R., Kulmala, M., 2005. Measurements in a highly polluted Asian mega city: observations of aerosol number size distribution, modal parameters and nucleation events. Atmospheric Chemistry and Physics 5, 57–66.

Mönkkönen, P., Uma, R., Srinivasan, D., Koponen, I.K., Lehtinen, K.E.J., Hämeri, K., Suresh, R., Sharma, V.P., Kulmala, M., 2004. Relationship and variations of

aerosol number and PM_{10} mass concentrations in a highly polluted urban environment—New Delhi, India. Atmospheric Environment 38, 425–433.
Mullen, N.A., Liu, C., Zhang, Y., Wang, S., Nazaroff, W.W. Ultrafine particle concentrations and exposures in four high-rise Beijing apartments. Atmospheric Environment, doi: 10.1016/j.atmosenv.2010.07.060, in press.
Narain, S., Roychowdhury, A., Mathur, H.B., Chattopadhyay, V., Chandola, P., Sen, J., 2010. Mobility Crisis: Agenda for Action 2010. Centre for Science and Environment, New Delhi, India, ISBN 978-81-86906-51-4.
Oberdörster, G., 2001. Pulmonary effects of inhaled ultrafine particles. International Archives of Occupational and Environmental Health 74, 1–8.
Ott, W., Klepeis, N., Switzer, P., 2008. Air change rates of motor vehicles and in-vehicle pollutant concentrations from secondhand smoke. Journal of Exposure Science and Environmental Epidemiology 18, 312–325.
Peters, A., von Klot, S., Heier, M., Trentinaglia, I., Hörmann, A., Wichmann, H.E., Löwel, H., 2004. Exposure to traffic and the onset of myocardial infarction. New England Journal of Medicine 351, 1721–1730.
Pope, C.A., Dockery, D.W., 2006. Health effects of fine particulate air pollution: lines that connect. Journal of the Air & Waste Management Association 56, 709–742.
Ramachandran, G., Adgate, J.L., Pratt, G.C., Sexton, K., 2003. Characterizing indoor and outdoor 15 minute average $PM_{2.5}$ concentrations in urban neighborhoods. Aerosol Science and Technology 37, 33–45.
Reynolds, C.C.O., Kandlikar, M., 2008. Climate impacts of air quality policy: switching to a natural gas-fueled public transportation system in New Delhi. Environmental Science & Technology 42, 5860–5865.
Reynolds, C.C.O., Kandlikar, M., Badami, M.G., 2011. Determinants of PM and GHG emissions from natural gas-fueled auto-rickshaws in Delhi. Transportation Research Part D: Transport and Environment 16, 160–165.
Riediker, M., Cascio, W.E., Griggs, T.R., Herbst, M.C., Bromberg, P.A., Neas, L., Williams, R.W., Devlin, R.B., 2004. Particulate matter exposure in cars is associated with cardiovascular effects in healthy young men. American Journal of Respiratory and Critical Care Medicine 169, 934–940.
Saksena, S., Prasad, R.K., Shankar, V.R., 2007. Daily exposure to air pollutants in indoor, outdoor and in-vehicle microenvironments: a pilot study in Delhi. Indoor and Built Environment 16, 39–46.
Tiwari, G., 2003. Transport and land-use policies in Delhi. Bulletin of the World Health Organization 81, 444–450.
US EPA, 2008. Air, in US EPA's 2008 Report on the Environment (Final Report). US Environmental Protection Agency, Washington, DC. Chapter 2 EPA/600/R-07/045F (NTIS PB2008–112484).
Westerdahl, D., Fruin, S., Sax, T., Fine, P.M., Sioutas, C., 2005. Mobile platform measurements of ultrafine particles and associated pollutant concentrations on freeways and residential streets in Los Angeles. Atmospheric Environment 39, 3597–3610.
Westerdahl, D., Wang, X., Pan, X., Zhang, K.M., 2009. Characterization of on-road vehicle emission factors and microenvironmental air quality in Beijing, China. Atmospheric Environment 43, 697–705.
Zhu, Y.F., Eiguren-Fernandez, A., Hinds, W.C., Miguel, A.H., 2007. In-cabin commuter exposure to ultrafine particles on Los Angeles freeways. Environmental Science & Technology 41, 2138–2145.

Supplementary Information

Concentrations of Fine, Ultrafine, and Black Carbon Particles in Auto-Rickshaws in New Delhi, India

Joshua S. Apte, Thomas W. Kirchstetter, Alexander H. Reich, Shyam J. Deshpande, Geetanjali Kaushik, Arvind Chel, Julian D. Marshall, and William W Nazaroff

Contents

SI.1 Methods

SI.1.1 Experiment to investigate self-pollution contribution to in-cabin exposures

We conducted an experiment to investigate potential entrainment of the auto-rickshaw's own exhaust into the passenger compartment (self-pollution). The test route was a 600 m single-lane loop that formed the perimeter of a forested park near the CRP site. Sampling was conducted on a weekend morning to minimize encounters with other vehicles. At the start of each circuit around the park, the auto-rickshaw paused with engine running for 1-2 min. After completing the loop (average speed: 14 km h^{-1}, maximum speed 18 km h^{-1}), the vehicle's engine was shut off immediately, and remained off for 1-2 min. This protocol (engine start, 1-2 min idle, drive loop, engine off 1-2 min) was repeated a total of 5 times. During the test, we continuously measured $PM_{2.5}$, BC, and PN concentrations using the same sampling methods described in §2 of the main

text. BC measurements were discarded due to instrument malfunction. Mean wind speed at CRP was 1.6 m s^{-1} during the test.

We did not find evidence of substantial self-pollution. The mean in-vehicle concentrations of $PM_{2.5}$ and PN were moderately lower than levels measured at CRP immediately following the self-pollution test (Figure SI.1). In-vehicle $PM_{2.5}$ and PN concentrations during the test did not indicate the large and frequent variability that was typical of our main exposure measurements (compare with Figure 2). Moreover, there was no pattern in pollutant concentrations that correlated with engine on/off status. We observed one PN spike of ~80×10^3 cm^{-3} midway through the second test iteration. The cause of this concentration spike is unclear, but we noted passing a two-stroke motorcycle at approximately the same time. The ratio of mean (median) concentration during periods with engine on to mean (median) concentration during periods with engine off was 1.02 (1.02) for $PM_{2.5}$ and 1.08 (0.99) for PN. An unpaired two-sample *t*-test indicated that the difference in mean pollutant concentration between periods with engine on and periods with engine off was statistically indistinguishable from zero ($p = 0.12$ for $PM_{2.5}$, $p = 0.34$ for PN). Overall, the results of this experiment are consistent with the hypothesis that the dominant contribution to in-vehicle concentrations along our main measurement route is from sources other than the auto-rickshaw in which we sampled.

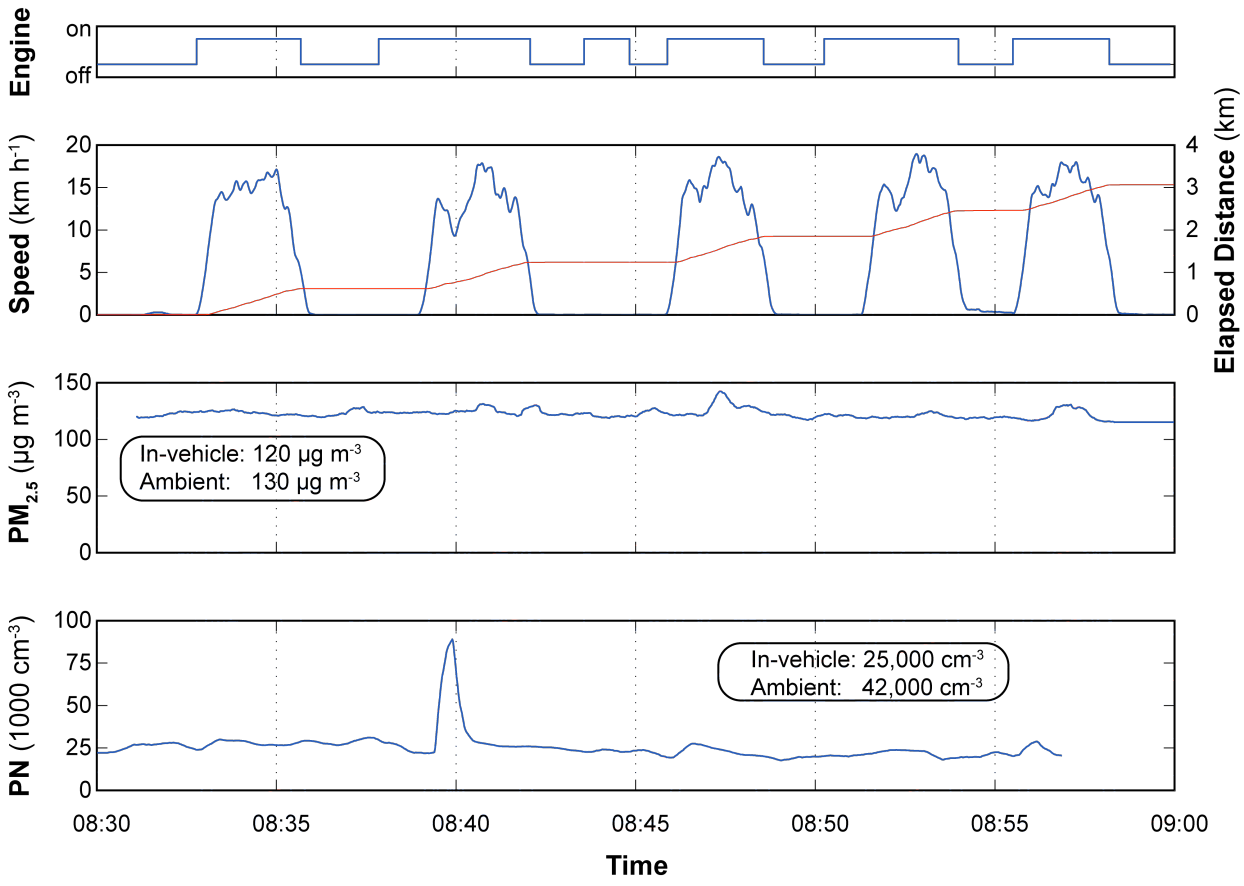

Figure SI.1. Traces of vehicle status and pollutant concentrations during an experiment to investigate potential self-pollution contribution to in-vehicle exposures. Engine on/off status was measured with a vibration transducer (Onset Corporation, Bourne, MA). Elapsed distance (red line) indicates the cumulative distance traveled around the ~ 600 m sampling loop over all iterations of the test. Note the relatively low and stable pollutant concentrations inside the auto-rickshaw (compare with Figure 2 in the main text).

SI.1.2 Gravimetric calibration of $PM_{2.5}$ measurements

To calibrate the DustTrak optical-to-mass response for New Delhi's aerosol, we developed a calibration relationship based on filter samples. A total of 36 gravimetric filter measurements were collected side-by-side with the DustTrak inside auto-rickshaws (16 samples) and at the Chittaranjan Park (CRP) ambient site (20 samples) between late March and early June 2010. We used an SKC PEM $PM_{2.5}$ impactor (MSP Corporation, Shoreview, MN) and an SKC Leland Legacy sampling pump operating at 10 L min^{-1} (SKC, Inc, Eighty Four, PA) to achieve a 2.5 µm

aerodynamic diameter size cut on the sample aerosol, which was collected on a preweighed 37-mm Teflon filters held by a rigid, porous backing plate. The median air volume sampled was 1.6 m^3 (10% trimmed range: 0.86 – 4.3 m^3).

Filter samples were conditioned for 24-72 hours before each weighing using a controlled chamber equilibrated to 35-45% RH and 22-25 ºC. Each filter was discharged of static electricity using a ^{210}Po source and weighed pre- and post-sampling on a 0.1 µg precision Sartorius SE-2 Microbalance (Sartorius AG, Göttingen, Germany) at Lawrence Berkeley National Laboratory (LBNL) in Berkeley, CA, USA. A total of 18 blank filters were retained for quality control, of which 3 were stored at LBNL, 11 were taken to India and returned unhandled, and 4 handling blanks were loaded and unloaded into the filter apparatus at the CRP ambient site but without turning on the pump. Of the 36 non-blank filters sampled, four were rejected during the post-sampling weighing session owing to visible damage, such as separation of the filter medium from its support ring, thereby yielding the 32 samples employed in analysis below.

Summary statistics for all filter weight changes are presented in Table SI.1. All blank filters recorded a loss in weight between the first and second weighing sessions (January 2010 and June 2010, respectively). To correct for this change in weight, we added the mean weight change for the handling blanks (8.5 µg) to each sample weight before calculating final gravimetric $PM_{2.5}$ concentrations.

We developed a calibration curve to represent the relationship between the gravimetric $PM_{2.5}$ concentration and the time-averaged, RH-corrected $PM_{2.5}$ concentrations reported by the colocated DustTrak. Figure SI.2 presents scatter plots of DustTrak and gravimetric $PM_{2.5}$ concentration measurements for the 32 valid sampling sessions. Exploratory data analysis revealed that simple linear regressions performed poorly in describing the relationship between

Table SI.1. Summary of sample and blank filter weight changes (μg). [a]

	Gravimetric samples (N = 32)	Blanks brought to India (N = 11)	Handling blanks (N = 4)	Blanks stored at LBNL (N = 3)
Min	30	-19	-15	-4.9
Median	230	-14	-7.7	-3.2
Mean	250	-13	-8.5	-3.5
Max	630	-5.3	-4.1	-2.4

[a] N = number of samples analyzed.

DustTrak and gravimetric $PM_{2.5}$ measurements, especially at relatively low ambient concentrations for Delhi (< 75 μg m^{-3}). We found that a power law regression relationship satisfactorily fit the observed data while also accommodating the zero calibration point:

$$G^* = a(D)^b \quad \text{(SI.1)}$$

Here, G^* is the modeled gravimetric $PM_{2.5}$ concentration (units: μg m^{-3}), D is the RH-corrected real-time DustTrak $PM_{2.5}$ concentration, and a and b are empirically determined fitting parameters via linear regression of the log-transformed data points. To account for the nonlinear behavior of the power law relationship, we used an iterative fitting algorithm and obtained the calibration relationship reported as equation 2 in the main text. Over all 60 sampling trips, the mean ratio of gravimetric-calibrated to RH-corrected $PM_{2.5}$ concentration was 0.74 for in-vehicle measurements, and 0.91 for ambient measurements. For the 32 individual filter samples, the root-mean-square error (RMSE) of the individual modeled gravimetric concentrations was 32 μg m^{-3} (coefficient of variation: 23%). We estimate the mean ± 95% CI bias of the calibration relationship to be 0 ± 9.1%. This uncertainty in the calibration relationship modestly reduces the precision of estimated mean $PM_{2.5}$ concentrations. Ratio comparisons between ambient and in-vehicle concentrations (γ, φ) are not affected by this uncertainty.

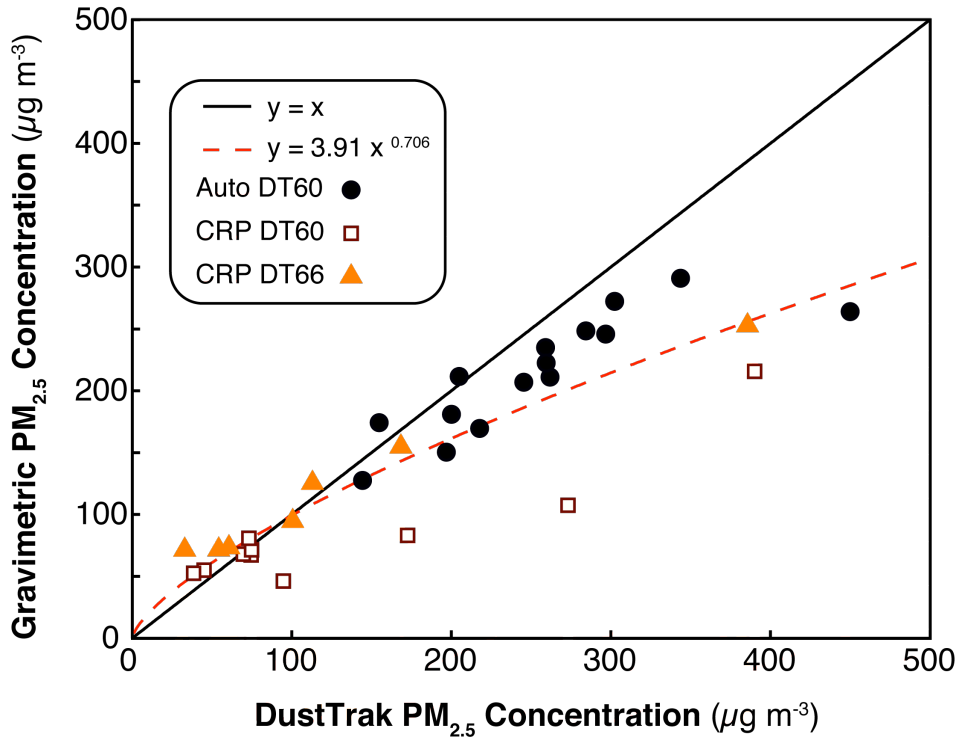

Figure SI.2. Scatter plot of colocated gravimetric and time-averaged DustTrak $PM_{2.5}$ concentration measurements. Points are plotted separately by measurement microenvironment ("auto" = auto-rickshaw, "CRP" = Chittaranjan Park ambient site) and by serial number of the TSI DustTrak used ("DT60", "DT66"). The dashed line indicates the best-fit calibration relationship.

SI.1.3 Post-processing of aethalometer black carbon measurements

SI.1.3.1 Removal of vibration-affected data points

We discovered early during field sampling that the Magee Scientific AE-51 "microAethalometer" instruments had strong sensitivity to mechanical shock and vibration that yielded spurious "spikes" in measured BC concentrations (Figure SI.3a). Controlled testing of the instrument in clean-air conditions revealed that sudden, forceful movement of the instrument caused a characteristic "spike" of ± 200 – 2000 μg m^{-3} that was typically short-lived (1-3 s). The pattern of spikes typically involved a very large positive and negative excursion in reported BC in close succession, within 1-3 s of each other. However, we found that the net contribution of a set of positive and negative BC concentration spikes typically *did not* average to zero over the

duration of each mechanical shock event. As this spurious signal likely introduces bias into the sample, we developed a post-processing algorithm to identify the characteristic signature of affected data points and exclude them from analysis. The algorithm identifies affected points by searching for instances of high relative deviation between an individual observation and surrounding data points, as follows:

1. Establish a moving baseline range of instrumental noise in the 1 Hz BC signal.
    a. For each 1-s observation compute the difference between each individual 1-s measurement of BC and the 30-s moving average of BC around that point. This time series is termed the "local deviation," or *LD*. For each time point *i,* the local deviation LD_i is computed as:

$$LD_i = BC_i^{raw} - \frac{1}{30}\sum_{i-15}^{i+14} BC_i^{raw} \quad \text{(SI.2)}$$

Here, BC_i^{raw} is the raw reported BC signal from the microAeth at time point *i*.

    b. For every 1-s observation, compute the 5-min moving-window 25th and 75th percentile of the local deviation time series generated by equation SI.2

$$LD_i^{5\,\mathrm{min},p75} = \mathrm{P}^{75}\left(LD_{i-150},\ldots,LD_{i+149}\right) \quad \text{(SI.3a)}$$

$$LD_i^{5\,\mathrm{min},p25} = \mathrm{P}^{25}\left(LD_{i-150},\ldots,LD_{i+149}\right) \quad \text{(SI.3b)}$$

Notation: the operator P^n computes the n^{th} percentile of a series. For example, $LD_i^{5\,\mathrm{min},p75}$ is the 75th percentile of the local deviation time series *LD*, evaluated over a 5-minute period of the *LD* time series centered on time point *i*, and extending over the 5 minutes (300 seconds) from point (*i* – 150) to point (*i* + 149).

2. Identify individual 1-s observations as "candidate extreme values" for exclusion if the local deviation (step 1a) of that observation is more than 5 times larger (smaller) than the 75th (25th) percentile of the 5-min moving-window instrumental noise, as calculated in step 1b:

$$CEV_i = \left\{ \begin{array}{l} IF\left(\begin{array}{l} \left[LD_i > \left(5 \times LD_i^{5\,\mathrm{min},p75} \right) \right] \\ OR\ \left[LD_i < \left(5 \times LD_i^{5\,\mathrm{min},p25} \right) \right] \end{array} \right), \text{ then } \quad TRUE \\ \qquad\qquad\qquad\qquad\qquad\qquad \ldots \text{ else } FALSE \end{array} \right\} \tag{SI.4}$$

Here, CEV_i represents whether an individual time point is determined to be a candidate extreme value ($CEV_i = TRUE$) or not ($CEV_i = FALSE$).

3. Search for negative BC concentrations within 2 s of each candidate extreme value identified in the previous step. Candidate extreme values that are negative or that have a negative BC measurement within ± 2 s are classified as spurious observations (SO). Each individual data point is evaluated for being a spurious observation with the following expression:

$$SO_i = \left\{ \begin{array}{l} IF\left(\begin{array}{l} \left(CEV_i = TRUE \right) \\ AND\left(\left[\sum_{i-2}^{i+2} \left(BC_i^{raw} < 0 \right) \right] > 0 \right) \end{array} \right), \text{ then } \quad TRUE \\ \qquad\qquad\qquad\qquad\qquad\qquad \ldots \text{else } FALSE \end{array} \right\} \tag{SI.5}$$

Here, SO_i represents whether an individual time point is determined to be a spurious observation ($SO_i = TRUE$) or not ($SO_i = FALSE$).

4. Remove each spurious BC observation and the other four BC observations within ± 2 s of the spurious value from analysis.

After applying this algorithm, we computed cleaned BC time series using the "sensor" and "reference" raw optical signals from the instrument, which measure the intensity of light (λ= 880 nm) transmitted through, respectively, the BC-laden filter spot and an area of filter unexposed to sample air. To remove inherent 1-s instrumental noise, we applied a 10-s moving average smoothing function to the sensor and reference optical signals, resulting in the variables I_S and I_R, respectively. Next, we computed BC concentrations for each observation at time $t = i$ using the following relations (Hansen et al., 1984):

$$I^*_{S_i} = I_{S_i}\left(I_{R_{i=1}} / I_{R_i}\right) \quad \text{(SI.6)}$$

$$\mathrm{d}ATN^*_i = -100 \ln\left(I^*_{S_i} / I^*_{S_{(i-1)}}\right) \quad \text{(SI.7)}$$

$$BC_i = \frac{A}{V_i}\left(\frac{\mathrm{d}ATN^*_i / 100}{\sigma}\right) \quad \text{(SI.8)}$$

In equation SI.6, I^*_{Si} represents the smoothed sensor beam signal at $t = i$, normalized for any change in the smoothed reference beam signal I_R between $t = 1$ and $t = i$. In equation SI.7, the instantaneous change in filter light attenuation dATN is computed using a Beer-Lambert type relation based on the change in instantaneous filter transmission. Equation SI.8 computes the instantaneous BC (units: g m^{-3}) concentration at $t = i$. Here, A represents the area of the filter spot (7.1×10^{-6} m^2), V_i represents the air volume swept through the filter between t = i-1 and $t = i$ (for 150 mL min^{-1} flow rate and 1 Hz data logging, $V = 2.5 \times 10^{-6}$ m^3), and σ is the attenuation coefficient, which for the manufacturer's default calibration is 12.5 m^2 g^{-1}. The effect of the cleaning algorithm is visible when comparing Figures SI.3a-c.

177 *SI.1.3.2 Adjustment of BC measurements for filter loading*

178 We further corrected BC measurements to account for the decreased instrumental sensitivity
179 to BC with increased filter loading based on the empirical calibration of Kirchstetter and
180 Novakov (2007) (see §2.2.3, equation 3, in the main text).

181

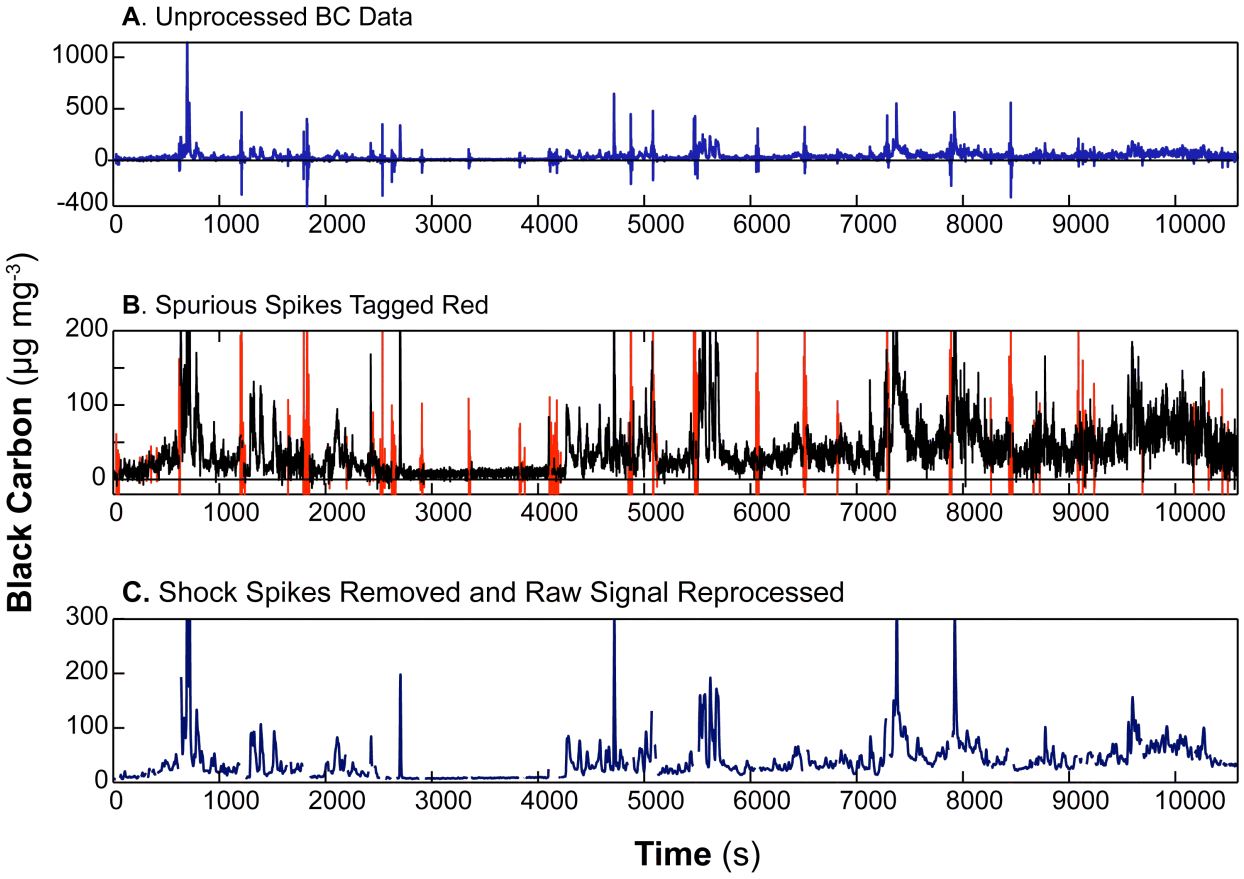

182

183 **Figure SI.3.** Effect of post-processing algorithm on aethalometer black carbon (BC) data. Raw data from
184 aethalometer is shown in (A), with extreme short-duration (1-3 s) excursions in measured BC evident.
185 These spurious measurements are detected by the post-processing algorithm and are identified in red color
186 in (B). The post-processed and smoothed time series is shown in (C).
187

188 Kirchstetter and Novakov attribute this effect to the true attenuation coefficient (σ, eq SI.8)
189 diminishing as filter transmission decreases (Tr), which corresponds with increased filter
190 loading. In contrast, the default manufacturer's calibration of the instrument implies that σ is not

affected by changes in filter loading. The coefficient values of 0.88 and 0.12 in equation 3 were empirically derived from laboratory experiments based on comparison of time-resolved aethalometer measurements with alternative non-filter based time-resolved methods and thermo-optical analysis of time-integrated filter samples (Kirchstetter and Novakov, 2007). As we collected a large set of colocated BC measurements with two separate microAethalometers, we were able to validate the choice of these particular coefficient values. Our study protocol included regular cross-comparison measurements between the two aethalometers (in-vehicle and at CRP) immediately before in-vehicle sampling, when filters in both instruments were clean. We repeated the same cross-comparison BC measurements immediately following in-vehicle sampling, when the instrument filters had differential BC mass loading.

For each pre- and post-trip comparison session, we computed the difference between the mean ambient BC concentrations measured by each instrument over the duration of the session. The median difference in concentration reported by the two instruments was close to zero for the pre-trip comparison sessions (Figure SI.4a). The effect of applying equation 3 was small for the pre-trip BC measurements, as both instruments started the session with fresh filters and therefore both had near-zero filter loading. In contrast, for post-trip measurements, filter loading was typically higher for the in-vehicle instrument than for the CRP ambient instrument, owing to higher on-roadway BC levels. As a result, the uncorrected post-trip ambient concentrations measured by the in-vehicle instrument were typically lower than the same concentrations measured simultaneously by the ambient site instrument (median difference: -2.7 $\mu g\ m^{-3}$ BC, Figure SI.4b). However, after correcting BC measurements for loading (equation 3), the median bias between the two instruments was reduced to nearly zero (median difference: -0.3 $\mu g\ m^{-3}$ BC

over ~43 comparison sessions). We conclude that equation 3 appropriately corrects for aethalometer loading effects.

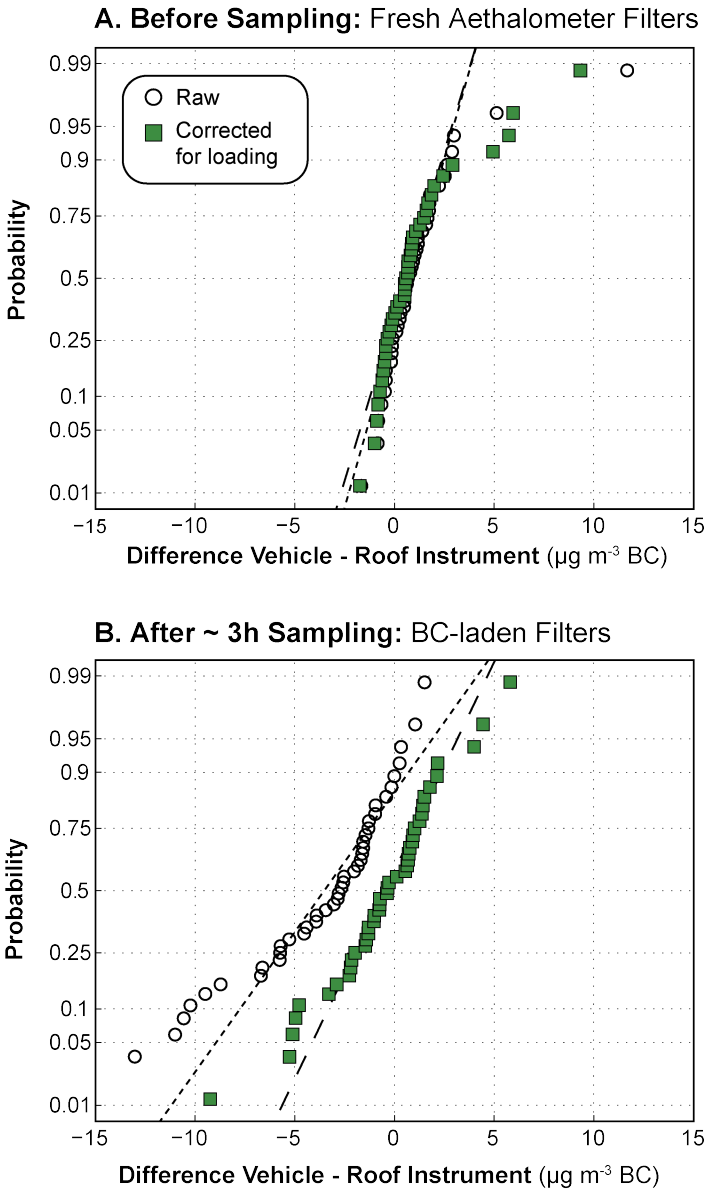

Figure SI.4. Effect of filter loading correction (equation 3) on colocated BC measurements. Horizontal axis is the difference in measured concentration at the CRP site between two instruments operating simultaneously: the instrument typically used for in-vehicle measurements, and the instrument typically used for rooftop CRP measurements. The vertical axis displays the cumulative probability of the distribution of differences. Note that the effect of correction is small for fresh filters (A), while the effect of the correction is more pronounced for BC-laden filters (B). For loaded filters, the median difference between colocated measurements after correction approaches zero (B).

SI.2 Results and Discussion

SI.2.1 Estimating coagulation timescale for ambient ultrafine particles

In §3.2, we suggest that the substantial elevation of on-road PN relative to urban background levels may be attributable to the dynamic loss mechanisms for ambient ultrafine particles (UFP). As previous work in New Delhi has identified coagulation as a possible sink for ambient ultrafine mode particles (Laakso et al., 2006; Mönkkönen et al., 2004; Mönkkönen et al., 2005), we present here calculations to demonstrate the plausibility of relatively rapid coagulation of ambient UFP. To estimate the coagulation timescale $\tau_{coag,i}$ for the coagulation of a single particle in size bin i with another particle, we used the following relation (Seinfeld and Pandis, 2006):

$$\tau_{coag,i} \sim \frac{1}{\sum_{j>10\,\mathrm{nm}} \beta_{i,j} N_j} \qquad \text{(SI.9)}$$

Here, $\beta_{i,j}$ represents the coagulation coefficient ($cm^3\ s^{-1}$) for a single particle in size bin i coagulating with particles in size bin j, and N_j (cm^{-3}) represents the number concentration of particles in size bin j. This version of the coagulation timescale equation allows for the possibility that the single particle will coagulate with either a larger or a smaller particle. As our particle counter only detects particles with $d_p > 10$ nm, we restrict the size of particles considered to those greater than 10 nm. We note that this form of the coagulation coefficient differs from another coagulation timescale, which evaluates the characteristic time for a particle of size i to coagulate with a particle of diameter larger than itself.

We computed $\beta_{i,j}$ using the Fuchs form of the Brownian coagulation coefficient (Seinfeld and Pandis, 2006) for $T = 20$ ºC. For these estimates, we employ the particle size distribution (PSD) for ambient air in New Delhi, as reported by Laakso et al. (2006) for October – November 2002. The distribution is idealized as the sum of three lognormal components (see Table SI.2).

Table SI.2. Sum-of-lognormals fit used to approximate New Delhi ambient particle size distribution (Laakso et al., 2006).

	N_{tot} (particles cm^{-3})	GMD (nm)	σ (-)
Nucleation mode	5150	11	1.4
Aitken mode	37930	44	1.8
Accumulation mode	22680	147	1.6

Using the PSD reported by Laakso et al., we estimate that $\tau_{coag,i}$ is in the range of 0.2 – 1.5 h for particles of diameter range 10 – 100 nm. Averaging over the entire PSD > 10 nm, we estimate that the mean coagulation timescale is ~ 1 h. However, the PN reported by Laakso et al. (2006) was ~ 68×10^3 particles cm^{-3}, roughly twice the level observed at the CRP ambient monitoring site during our measurements. To evaluate the effect of lower ambient concentrations, we scaled down the number concentration of each size bin of the PSD so that the total PN was equivalent to the mean ambient PN concentration we measured, 35×10^3 particles cm^{-3}. Doing so resulted in longer coagulation time scales, with a range of ~ 0.3 – 3 h for particles in the size range of 10 – 100 nm. Averaged over all particle sizes > 10 nm in the rescaled PSD, we estimate that the mean coagulation timescale is ~ 2 h at this lower concentration. We conclude that coagulation is a significant sink for ambient PN in New Delhi, since the coagulation time scales we have estimated are shorter than the urban-air residence time of ~ 5-15 h, based on the ratio of the urban length scale, 40-50 km, to the typical 1-2 m s^{-1} near-surface wind speed.

SI.2.2 Seasonal and temporal variation in ambient concentrations

We used unbalanced two-way ANOVA to decompose variability in ambient $PM_{2.5}$, BC, and PN measured concentrations into seasonal (month) and temporal (AM trip/ PM trip) components (Figure SI.5). Holding time of day constant, there was a statistically significant declining trend in ambient levels for all three pollutants during the February – May study period. The decline was

most pronounced for $PM_{2.5}$ and BC. We speculate that the observed decrease in ambient concentrations is partially attributable to Delhi's seasonally dependent patterns of 1) atmospheric mixing and 2) emissions from solid fuel combustion for heat. In addition to the seasonal trends, there was a statistically significant time-of-day trend for ambient $PM_{2.5}$ levels throughout the study period. Evening commute-time (6-9 PM) ambient concentrations were typically lower than morning (9 AM – noon) commute-time ambient concentrations (median difference: ~25%). We did not detect statistically significant differences in ambient BC and PN concentrations between AM and PM commute hours.

SI.2.3 Comparing results with studies from elsewhere

Table SI.3 provides quantitative documentation for Figure 7 in the main article, which compares the measured results from this study with the concentrations reported by other studies elsewhere. Our survey of the literature is not exhaustive, but it is indicative of the range of exposure concentrations in transportation microenvironments in urban areas around the world.

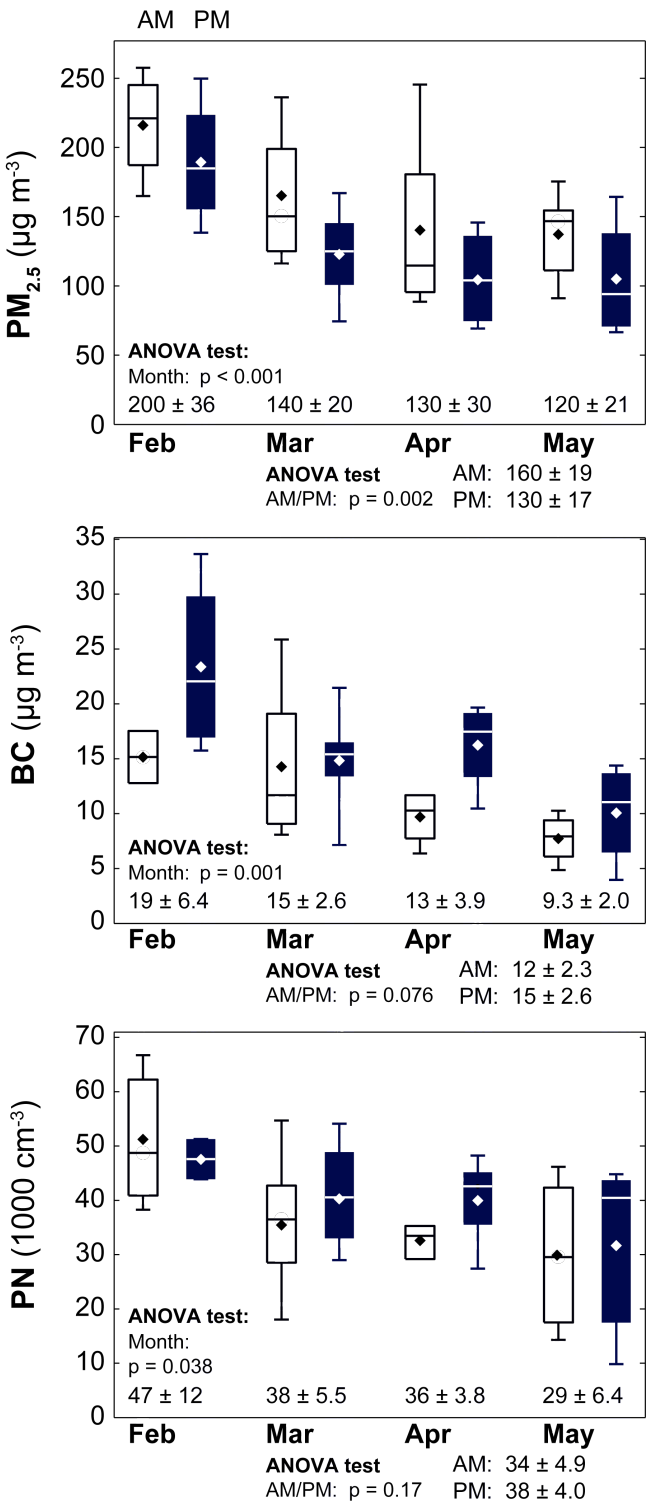

Figure SI.5. ANOVA decomposition of variability in ambient concentrations into month-of-year and time-of-day components.

288

Table SI.3. Comparison of present study results with prior measurements in megacities and elsewhere. [a]

Exposure Studies

Study	City/Microenvironment	Year	Hours	$PM_{2.5}$ (μg m^{-3})		BC (μg m^{-3})		PN (10^3 cm^{-3}) [c]	
				Ambient	Vehicle	Ambient	Vehicle	Ambient	Vehicle
Present study	**New Delhi, India**								
	Auto-Rickshaw	2010	~160	140	190	10	43	$35^{(10)}$	$280^{(10)}$
	Car (AC / Non AC)		~20	120	110, 170	9	29, 49	$30^{(10)}$	$100, 180^{(10)}$
Kaur et al., 2005	**London, UK**	2003							
	Car / Arterial			9.9	38	-	-	-	$100^{(20)}$
	Bus / Arterial			-	35	-	-	-	$100^{(20)}$
	Bicycle / Arterial			-	34	-	-	-	$94^{(20)}$
Boogaard et al., 2009	**11 Dutch Cities**	2006	~30						
	Car / Arterial			-	49 [b]	-	-	$\sim10^{(10)}$	$26^{(10)}$
	Bicycle / Cycle Path			-	44 [b]	-	-	$\sim10^{(10)}$	$24^{(10)}$
Knibbs and de Dear, 2010	**Sydney, Australia**	2004							
	Bus			-	30 [b]	-	-	-	$84^{(10)}$
	Car			-	22 [b]	-	-	-	$75^{(10)}$
Chan et al., 2002	**Hong Kong, China**	2000							
	Bus (AC / Non AC)			-	51, 93	-	-	-	-
	Tram (on roadway)			-	110	-	-	-	-

On-Road Concentration Studies

Study	City / Microenvironment	Year	Hours	$PM_{2.5}$ (μg m^{-3})		BC (μg m^{-3})		PN (10^3 cm^{-3}) [c]	
				Ambient	On-road	Ambient	On-road	Ambient	On-road
Westerdahl et al., 2009	**Beijing, China**								
	BJ - *Arterials / Day-LDV*	2007	~10	-	-	3.4	22	$27^{(6)}$	$82^{(6)}$
	BJ* - *Arterials / Night-HDV*			-	-	11	60	$19^{(6)}$	$290^{(6)}$
Fruin et al., 2008	**Los Angeles, USA**								
	LA - *Residential/LDV*	2003	~15	7.9	23	0.74	1.5	$13^{(7)}$	$33^{(7)}$
	LA* - *Urban/HDV*			17	54	1.5	12	$26^{(7)}$	$190^{(7)}$
Kittelson et al., 2004	**Minneapolis, USA**								
	Freeways	2003	~20	-	-	-	-	$9.4^{(3)}$	$400^{(3)}$
Bukowiecki et al., 2003	**Zürich, Switzerland**								
	Arterials	2000	~5	-	-	-	-	$5\text{-}15^{(3)}$	$30\text{-}50^{(3)}$

[a] Values are central tendency results from each study (geometric mean when available, otherwise arithmetic mean). Abbreviations: "$PM_{2.5}$" – fine particle mass, "BC" – black carbon, "PN" – particle number concentration, "LDV" – light-duty vehicle, "HDV" – heavy-duty vehicle.

[b] TSI DustTrak aerosol photometer used without adjustment for humidity or mass-based calibration against local aerosol, indicating possible overestimate.

[c] Superscripts on PN concentrations indicate minimum particle diameter (nm) detected by instrument for given study.

References

Boogaard, H., Borgman, F., Kamminga, J., Hoek, G., 2009. Exposure to ultrafine and fine particles and noise during cycling and driving in 11 Dutch cities. Atmospheric Environment 43, 4234-4242.

Bukowiecki, N., Dommen, J., Prévôt, A.S.H., Weingartner, E., Baltensperger, U., 2003. Fine and ultrafine particles in the Zürich (Switzerland) area measured with a mobile laboratory: an assessment of the seasonal and regional variation throughout a year. Atmopheric Chemistry and Physics 3, 1477-1494.

Chan, L.Y., Lau, W.L., Lee, S.C., Chan, C.Y., 2002. Commuter exposure to particulate matter in public transportation modes in Hong Kong. Atmospheric Environment 36, 3363-3373.

Fruin, S., Westerdahl, D., Sax, T., Sioutas, C., Fine, P.M., 2008. Measurements and predictors of on-road ultrafine particle concentrations and associated pollutants in Los Angeles. Atmospheric Environment 42, 207-219.

Hansen, A.D.A., Rosen, H., Novakov, T., 1984. The aethalometer - An instrument for the real-time measurement of optical absorption by aerosol particles. Science of the Total Environment 36, 191-196.

Kaur, S., Nieuwenhuijsen, M., Colvile, R., 2005. Personal exposure of street canyon intersection users to $PM_{2.5}$, ultrafine particle counts and carbon monoxide in Central London, UK. Atmospheric Environment 39, 3629-3641.

Kirchstetter, T.W., Novakov, T., 2007. Controlled generation of black carbon particles from a diffusion flame and applications in evaluating black carbon measurement methods. Atmospheric Environment 41, 1874-1888.

Kittelson, D.B., Watts, W.F., Johnson, J.P., 2004. Nanoparticle emissions on Minnesota highways. Atmospheric Environment 38, 9-19.

Knibbs, L.D., de Dear, R.J., 2010. Exposure to ultrafine particles and $PM_{2.5}$ in four Sydney transport modes. Atmospheric Environment 44, 3224-3227.

Laakso, L., Koponen, I.K., Mönkkönen, P., Kulmala, M., Kerminen, V.M., Wehner, B., Wiedensohler, A., Wu, Z., Hu, M., 2006. Aerosol particles in the developing world; a

comparison between New Delhi in India and Beijing in China. Water, Air, and Soil Pollution 173, 5-20.

Mönkkönen, P., Koponen, I.K., Lehtinen, K.E.J., Hämeri, K., Uma, R., Kulmala, M., 2005. Measurements in a highly polluted Asian mega city: observations of aerosol number size distribution, modal parameters and nucleation events. Atmospheric Chemistry and Physics 5, 57-66.

Mönkkönen, P., Uma, R., Srinivasan, D., Koponen, I.K., Lehtinen, K.E.J., Hämeri, K., Suresh, R., Sharma, V.P., Kulmala, M., 2004. Relationship and variations of aerosol number and PM_{10} mass concentrations in a highly polluted urban environment—New Delhi, India. Atmospheric Environment 38, 425-433.

Seinfeld, J.H., Pandis, S.N., 2006. Atmospheric Chemistry and Physics, Second Edition. Wiley-Interscience, Hoboken, NJ, Chapter 13.

Westerdahl, D., Wang, X., Pan, X., Zhang, K.M., 2009. Characterization of on-road vehicle emission factors and microenvironmental air quality in Beijing, China. Atmospheric Environment 43, 697-705.